AN ADAPTIVE FINITE ELEMENT DtN METHOD FOR THE ELASTIC WAVE SCATTERING PROBLEM IN THREE DIMENSIONS*

GANG BAO†, PEIJUN LI‡, AND XIAOKAI YUAN†§

Abstract. Consider the elastic scattering of an incident wave by a rigid obstacle in three dimensions, which is formulated as an exterior problem for the Navier equation. By constructing a Dirichlet-to-Neumann (DtN) operator and introducing a transparent boundary condition, the scattering problem is reduced equivalently to a boundary value problem in a bounded domain. The discrete problem with the truncated DtN operator is solved by using the a posteriori error estimate based adaptive finite element method. The estimate takes account of both the finite element approximation error and the truncation error of the DtN operator, where the latter is shown to converge exponentially with respect to the truncation parameter. Moreover, the generalized Woodbury matrix identity is utilized to solve the resulting linear system efficiently. Numerical experiments are presented to demonstrate the superior performance of the proposed method.

Key words. elastic wave equation, obstacle scattering problem, Dirichlet-to-Neumann operator, transparent boundary condition, adaptive finite element method, a posteriori error estimate

AMS subject classifications. 65N30, 65N12, 78A45

DOI. 10.1137/21M1392000

1. Introduction. A basic problem in classical scattering theory, the obstacle scattering problem refers to the scattering of a time-harmonic wave by an impenetrable medium of compact support. It plays a fundamental role in diverse scientific areas such as radar and sonar, geophysical exploration, medical imaging, and nondestructive testing. Obstacle scattering problems have been extensively investigated in both the engineering and mathematical communities. A great number of numerical and mathematical results are available, especially for acoustic and electromagnetic waves [9, 31, 32]. Recently, the scattering problems for elastic waves have received everincreasing attention due to the significant applications in geophysics, seismology, and elastography [2, 6, 7, 26]. Compared to work on acoustic and electromagnetic waves, in the research on scattering problems for elastic waves, there remain many unresolved issues on theoretical analysis and numerical computation because of the complexity of the model equation [8, 24].

The elastic obstacle scattering problem is imposed in an unbounded domain, which needs to be truncated into a bounded one when applying domain discretization based numerical methods. Therefore, an appropriate boundary condition is required on the boundary of the truncated domain so that no artificial wave reflection occurs. Such a boundary condition is called a nonreflecting boundary condition or transparent boundary condition (TBC). Despite the large amount of work done so far, developing effective nonreflecting boundary conditions in the area of

^{*}Received by the editors January 14, 2021; accepted for publication (in revised form) August 26, 2021; published electronically November 18, 2021.

https://doi.org/10.1137/21M1392000

Funding: The first author was partially supported by the NSFC Innovative Group Fund, grant 11621101. The second author was supported in part by NSF grant DMS-1912704.

[†]School of Mathematical Sciences, Zhejiang University, Hangzhou, Zhejiang 310027, China (baog@zju.edu.cn, yuan170@zju.edu.cn).

 $^{^{\}ddagger} \text{Department}$ of Mathematics, Purdue University, West Lafayette, IN 47907 USA (lipeijun@math.purdue.edu).

 $^{^{\}S}$ Current address: School of Mathematics, Jilin University, Changchun, Jilin 130012, People's Republic of China.

computational wave propagation remains an important and active research subject [5, 11, 13, 14, 15, 16, 17, 20, 36]. In this work, we construct a Dirichlet-to-Neumann (DtN) operator and develop a TBC for solving the elastic obstacle scattering problem in three dimensions. Based on the Helmholtz decomposition, the scattered field of the elastic displacement is split into the compressional and shear wave components, which satisfy the Helmholtz equation and the Maxwell equation, respectively. Therefore, the DtN operator for the elastic wave equation can be obtained from the well-studied DtN operators for the Helmholtz and Maxwell equations. Since the TBC is exact, the artificial boundary could be put as close as possible to the obstacle so as to reduce the computational complexity [23, 29].

To design an efficient numerical method, there are two more issues which need to be addressed. The first issue concerns the truncation of the DtN operator. The nonlocal DtN operator is given as an infinite series, which has to be truncated into a sum of finitely many terms in actual computation. However, it is known that the convergence of the truncated DtN operator could be arbitrarily slow in the operator norm [19]. From the computational viewpoint, it is important to answer the question of how many terms are required in order to maintain a certain level of accuracy. Second, the solution may have local singularity when the obstacle has edges. The mesh should be fine around the nonsmooth part of the obstacle in order to capture the singularity of the solution, while the mesh could be coarse in other parts of the domain where the solution is smooth. Hence, it is crucial to design an algorithm for mesh modification which can equally distribute the computational effort and optimize the computation.

In this paper, we propose an a posteriori error estimate based adaptive finite element method with the truncated DtN operator to overcome the two difficulties. Specifically, we consider the scattering of an incident wave by a rigid obstacle in three dimensions. The exterior domain is assumed to be filled with a homogeneous and isotropic elastic medium. The elastic wave propagation is governed by the Navier equation. Based on the TBC, the exterior scattering problem is formulated equivalently into a boundary value problem in a bounded domain. The discrete problem is solved by using the finite element method with the truncated DtN operator. A new duality argument is developed by using the Helmholtz decomposition to obtain an a posteriori error estimate between the solutions of the original scattering problem and the discrete problem. The estimate takes account of both the finite element approximation error and the truncation error of the DtN operator, where the latter is shown to decay exponentially with respect to the truncation parameter. The estimate is used to design the adaptive finite element algorithm to choose elements for refinements and to determine the truncation parameter. The stiffness matrix is made of a sparse, real, and symmetric matrix, which comes from the discretization of the variational formulation in the interior of the domain, and a dense low rank matrix given by vector products, which arises from the nonlocal TBC. The generalized Woodbury matrix identity is utilized to solve the resulting linear system efficiently. Numerical experiments are presented to demonstrate the superior performance of the proposed method.

Recently, the adaptive finite element DtN method has been developed to solve many acoustic and electromagnetic scattering problems, such as obstacle scattering problems [3, 21], diffraction grating problems [22, 35], and open cavity scattering problems [38]. This paper is a nontrivial extension of our previous work on the two-dimensional elastic obstacle scattering problem [28]. Apparently, the analysis is more sophisticated and the computation is more intensive for the three-dimensional prob-

lem. This work adds a significant contribution to designing efficient computational methods for solving elastic wave scattering problems.

The paper is organized as follows. In section 2, the elastic wave equation is introduced, the boundary value problem is formulated by using the TBC, and the corresponding weak formulation is discussed. In section 3, the discrete problem is considered by using the finite element approximation with the truncated DtN operator. Section 4 is devoted to the a posteriori error analysis and serves as the basis of the adaptive algorithm. In section 5, we discuss the numerical implementation of the adaptive algorithm, the construction of the stiffness matrix, and an efficient solver for the linear system; two numerical examples are presented to illustrate the performance of the proposed method. The paper concludes with some general remarks in section 6.

2. Problem formulation. Let $D \subset \mathbb{R}^3$ be an elastically rigid obstacle with Lipschitz continuous boundary ∂D . Denote by ν the unit outward normal vector on ∂D . The exterior domain $\mathbb{R}^3 \setminus \overline{D}$ is assumed to be filled with a homogeneous and isotropic elastic medium with a unit mass density. Let $B_R = \{x \in \mathbb{R}^3 : |x| < R\}$ and $B_{R'} = \{x \in \mathbb{R}^3 : |x| < R'\}$ be balls with radii R and R', where 0 < R' < R. Denote by Γ_R and $\Gamma_{R'}$ the surfaces of B_R and $B_{R'}$, respectively. Let $\Omega = B_R \setminus \overline{D}$ be the bounded domain enclosed by the surfaces ∂D and Γ_R .

Let the obstacle be illuminated by an incident wave u^{inc} , which can be either a plane wave or a point source. The displacement of the total field u satisfies the elastic wave equation

(2.1)
$$\mu \Delta \boldsymbol{u} + (\lambda + \mu) \nabla \nabla \cdot \boldsymbol{u} + \omega^2 \boldsymbol{u} = 0 \quad \text{in } \mathbb{R}^3 \setminus \overline{D},$$

where $\omega > 0$ is the angular frequency and λ, μ are the Lamé constants satisfying $\mu > 0, 3\lambda + 2\mu > 0$. Since the obstacle is assumed to be elastically rigid, the total field vanishes on the surface of the obstacle

$$\mathbf{u} = 0$$
 on ∂D .

Introduce the Helmholtz decomposition

(2.2)
$$\mathbf{u} = \nabla \phi + \nabla \times \mathbf{\psi}, \quad \nabla \cdot \mathbf{\psi} = 0.$$

Substituting (2.2) into (2.1), we may verify that the potentials ϕ and ψ satisfy the Helmholtz equation and the Maxwell equation in $\mathbb{R}^3 \setminus \overline{D}$, respectively, i.e.,

$$\Delta \phi + \kappa_p^2 \phi = 0, \quad \nabla \times (\nabla \times \psi) - \kappa_s^2 \psi = 0,$$

where $\kappa_p = \omega/(\lambda + 2\mu)^{1/2}$ and $\kappa_s = \omega/\mu^{1/2}$ are known as the compressional wavenumber and the shear wavenumber, respectively.

Denote the scattered field $\boldsymbol{u}^s = \boldsymbol{u} - \boldsymbol{u}^{\text{inc}}$, and let ϕ^s and $\boldsymbol{\psi}^s$ be the potential functions of the Helmholtz decomposition for the scattered field \boldsymbol{u}^s . It is required that ϕ^s and $\boldsymbol{\psi}^s$ satisfy the Sommerfeld radiation condition and the Silver-Müller radiation condition, respectively, i.e.,

$$\lim_{\rho \to \infty} \rho \left(\partial_{\rho} \phi^{s} - i \kappa_{p} \phi^{s} \right) = 0, \quad \lim_{\rho \to \infty} \left((\nabla \times \boldsymbol{\psi}^{s}) \times \boldsymbol{x} - i \kappa_{s} \rho \boldsymbol{\psi}^{s} \right) = 0, \quad \rho = |\boldsymbol{x}|.$$

The obstacle scattering problem is defined in the unbounded domain $\mathbb{R}^3 \setminus \overline{D}$. It needs to be reduced into the bounded domain Ω . Next we introduce a TBC on Γ_R . The

details can be found in the accompanying supplementary material file supplement.pdf [local/web 314KB]. Define a boundary operator for the displacement of the scattered wave

(2.3)
$$\mathscr{D} \boldsymbol{u}^s := \mu \partial_{\rho} \boldsymbol{u}^s + (\lambda + \mu)(\nabla \cdot \boldsymbol{u}^s) \boldsymbol{e}_{\rho} \quad \text{on } \Gamma_R.$$

In the spherical coordinates, the scattered field admits the following expansion on Γ_R :

$$\boldsymbol{u}^{s}(R,\theta,\varphi) = \sum_{n=0}^{\infty} \sum_{m=-n}^{n} u_{1n}^{sm} \boldsymbol{U}_{n}^{m}(\theta,\varphi) + u_{2n}^{sm} \boldsymbol{V}_{n}^{m}(\theta,\varphi) + u_{3n}^{sm} X_{n}^{m}(\theta,\varphi) \boldsymbol{e}_{\rho}.$$

Introduce the DtN operator \mathcal{T} , and the TBC is imposed as

(2.4)
$$\mathscr{D}\boldsymbol{u}^{s} = \mathscr{T}\boldsymbol{u}^{s} := \sum_{n=0}^{\infty} \sum_{m=-n}^{n} b_{1n}^{m} \boldsymbol{U}_{n}^{m} + b_{2n}^{m} \boldsymbol{V}_{n}^{m} + b_{3n}^{m} \boldsymbol{X}_{n}^{m} \boldsymbol{e}_{\rho} \quad \text{on } \Gamma_{R},$$

where the Fourier coefficients $\boldsymbol{b}_n^m = (b_{1n}^m, b_{2n}^m, b_{3n}^m)^{\top}$ and $\boldsymbol{u}_n^{sm} = (u_{1n}^{sm}, u_{2n}^{sm}, u_{3n}^{sm})^{\top}$ are connected by $\boldsymbol{b}_n^m = M_n \boldsymbol{u}_n^{sm}$. Here M_n is a 3×3 matrix, and all of its elements can be found in SM4. Since $\boldsymbol{u} = \boldsymbol{u}^s + \boldsymbol{u}^{\text{inc}}$, the TBC for the total field is

$$\mathscr{D}\boldsymbol{u} = \mathscr{T}\boldsymbol{u} + \boldsymbol{g}.$$

where $g := \mathscr{D} u^{\mathrm{inc}} - \mathscr{T} u^{\mathrm{inc}}$.

Based on (2.5), the scattering problem can be reformulated as the following variational problem: find $\mathbf{u} \in \mathbf{H}_{\partial D}^1(\Omega)$ such that

(2.6)
$$b(\boldsymbol{u}, \boldsymbol{v}) = \int_{\Gamma_R} \boldsymbol{g} \cdot \overline{\boldsymbol{v}} ds \quad \forall \, \boldsymbol{v} \in \boldsymbol{H}^1_{\partial D}(\Omega),$$

where the sesquilinear form $b: \mathbf{H}^1_{\partial D}(\Omega) \times \mathbf{H}^1_{\partial D}(\Omega) \to \mathbb{C}$ is defined as

$$b(\boldsymbol{u}, \boldsymbol{v}) = \mu \int_{\Omega} \nabla \boldsymbol{u} : \nabla \overline{\boldsymbol{v}} d\boldsymbol{x} + (\lambda + \mu) \int_{\Omega} (\nabla \cdot \boldsymbol{u}) (\nabla \cdot \overline{\boldsymbol{v}}) d\boldsymbol{x}$$
$$-\omega^{2} \int_{\Omega} \boldsymbol{u} \cdot \overline{\boldsymbol{v}} d\boldsymbol{x} - \int_{\Gamma_{R}} \mathscr{T} \boldsymbol{u} \cdot \overline{\boldsymbol{v}} ds.$$

Here $A: B = \operatorname{tr}(AB^{\top})$ is the Frobenius inner product of square matrices A and B. It is shown in [27] that the variational problem admits a unique weak solution $\boldsymbol{u} \in \boldsymbol{H}_{\partial D}^{1}(\Omega)$, which satisfies the estimate

(2.7)
$$\|u\|_{H^{1}(\Omega)} \lesssim \|g\|_{H^{-1/2}(\Gamma_{R})} \lesssim \|u^{\text{inc}}\|_{H^{1}(\Omega)}.$$

Hereafter, the notation $a \lesssim b$ stands for $a \leq Cb$, where C > 0 is a generic constant whose value is not required and may change step by step in the proofs.

Since the variational problem is well-posed, we have from the general theory in [1] that there exists a constant $\gamma > 0$ such that the following inf-sup condition holds:

$$\sup_{0\neq \boldsymbol{v}\in \boldsymbol{H}_{\partial D}^{1}(\Omega)}\frac{|b(\boldsymbol{u},\boldsymbol{v})|}{\|\boldsymbol{v}\|_{\boldsymbol{H}^{1}(\Omega)}}\geq \gamma\|\boldsymbol{u}\|_{\boldsymbol{H}^{1}(\Omega)}\quad\forall\,\boldsymbol{u}\in \boldsymbol{H}_{\partial D}^{1}(\Omega).$$

Remark 2.1. As an alternative to (2.3), the following traction operator may be adopted to handle the TBC:

$$\mathscr{D}\boldsymbol{u} = 2\mu\partial_{\boldsymbol{\nu}}\boldsymbol{u} + \lambda(\nabla\cdot\boldsymbol{u})\boldsymbol{\nu} + \mu\boldsymbol{\nu}\times(\nabla\times\boldsymbol{u}).$$

Although the traction operator will change the specific form of the DtN operator and the variational formulation, the analysis can be similarly carried out for the a posteriori error estimate.

3. The discrete problem. Given a sufficiently large N, define the truncated DtN operator

(3.1)
$$\mathscr{T}_{N} \boldsymbol{u} = \sum_{n=0}^{N} \sum_{m=-n}^{n} b_{1n}^{m} \boldsymbol{U}_{n}^{m} + b_{2n}^{m} \boldsymbol{V}_{n}^{m} + b_{3n}^{m} \boldsymbol{X}_{n}^{m} \boldsymbol{e}_{\rho}.$$

In practice, g has to be approximated by $g_N := \mathcal{D} u^{\text{inc}} - \mathcal{T}_N u^{\text{inc}}$. The truncated variational problem is to find $u_N \in H^1_{\partial D}(\Omega)$ such that

(3.2)
$$b_N(\boldsymbol{u}_N, \boldsymbol{v}) = \int_{\Gamma_R} \boldsymbol{g}_N \cdot \overline{\boldsymbol{v}} ds \quad \forall \, \boldsymbol{v} \in \boldsymbol{H}^1_{\partial D}(\Omega),$$

where the sesquilinear form $b_N: H^1_{\partial D}(\Omega) \times H^1_{\partial D}(\Omega) \to \mathbb{C}$ is given by

$$b_{N}(\boldsymbol{u},\boldsymbol{v}) = \mu \int_{\Omega} \nabla \boldsymbol{u} : \nabla \overline{\boldsymbol{v}} d\boldsymbol{x} + (\lambda + \mu) \int_{\Omega} (\nabla \cdot \boldsymbol{u}) (\nabla \cdot \overline{\boldsymbol{v}}) d\boldsymbol{x}$$
$$-\omega^{2} \int_{\Omega} \boldsymbol{u} \cdot \overline{\boldsymbol{v}} d\boldsymbol{x} - \int_{\Gamma_{R}} \mathscr{T}_{N} \boldsymbol{u} \cdot \overline{\boldsymbol{v}} ds.$$

Let \mathcal{M}_h be a regular tetrahedral mesh of Ω , where h denotes the maximum diameter of all the elements in \mathcal{M}_h . For simplicity, we assume that the surfaces ∂D and Γ_R are polyhedral and ignore the approximation error on the surfaces, which allows us to focus on deducing the a posteriori error estimate. Thus any face $e \in \mathcal{M}_h$ is a subset of $\partial \Omega$ if it has three boundary vertices. Let $\tilde{\boldsymbol{V}}_h \subset \boldsymbol{H}^1(\Omega)$ be a conforming finite element space, i.e.,

$$\tilde{\boldsymbol{V}}_h := \left\{ \boldsymbol{v} \in C(\overline{\Omega})^3 : \boldsymbol{v}|_T \in P_m(T)^3 \ \forall T \in \mathcal{M}_h \right\},$$

where m is a positive integer and $P_m(T)$ denotes the set of all polynomials of degree no more than m. We introduce an isoparametric-equivalent finite element space [25]:

$$oldsymbol{V}_h := \left\{ oldsymbol{v}(oldsymbol{F}^{-1}(oldsymbol{x})) : oldsymbol{x} \in oldsymbol{F}(\Omega_h), oldsymbol{v} \in ilde{oldsymbol{V}}_h
ight\},$$

where F is a one-to-one continuous mapping which maps the polyhedral surface exactly on the spherical surface. The finite element approximation to the variational problem (3.2) is to find $\boldsymbol{u}_N^h \in \boldsymbol{V}_{h,\partial D}$ such that

(3.3)
$$b_N(\boldsymbol{u}_N^h, \boldsymbol{v}_N^h) = \int_{\Gamma_R} \boldsymbol{g}_N \cdot \overline{\boldsymbol{v}}_N^h ds \quad \forall \, \boldsymbol{v}^h \in \boldsymbol{V}_{h,\partial D},$$

where $V_{h,\partial D} = \{ v \in V_h : v = 0 \text{ on } \partial D \}.$

Following the idea in [19] and the discussion of [27], we may show that for sufficiently large N the variational problem (3.2) is well-posed. Meanwhile, for sufficiently small h, the discrete inf-sup condition of the sesquilinear form b_N may also be established by following the approach in [33]. Based on the general theory in [1], the truncated variational problem (3.3) can be shown to have a unique solution $u_N^h \in V_h$. The details are omitted since our focus is the a posteriori error estimate and the convergence analysis for the truncated DtN operator.

4. The a posteriori error analysis. For any tetrahedral element $T \in \mathcal{M}_h$, denote by h_T its diameter. Let \mathcal{B}_F denote the set of all the faces of T and h_F be the size of the face F. For any interior face F which is the common face of tetrahedral element $T_1, T_2 \in \mathcal{M}_h$, define the jump residual across F as

$$J_F = -\left[\mu \nabla \boldsymbol{u}_N^h \cdot \nu_1 + (\lambda + \mu)(\nabla \cdot \boldsymbol{u}_N^h)\nu_1 + \mu \nabla \boldsymbol{u}_N^h \cdot \nu_2 + (\lambda + \mu)(\nabla \cdot \boldsymbol{u}_N^h)\nu_2\right],$$

where ν_j is the unit outward normal vector on the boundary of T_j , j=1,2. For any boundary edge $F \subset \Gamma_R$, the jump residual is

$$J_F = 2 \left(\mathscr{T}_N \boldsymbol{u}_N^h + \boldsymbol{g}_N - \mu \nabla \boldsymbol{u}_N^h \cdot \boldsymbol{e}_\rho - (\lambda + \mu) (\nabla \cdot \boldsymbol{u}_N^h) \boldsymbol{e}_\rho \right).$$

For any tetrahedral element $T \in \mathcal{M}_h$, define the local error estimator as

$$\eta_T = h_T \| \mathscr{R} \boldsymbol{u}_N^h \|_{\boldsymbol{L}^2(T)} + \left(\frac{1}{2} \sum_{F \in \partial T} h_F \| J_F \|_{\boldsymbol{L}^2(F)}^2 \right)^{1/2},$$

where \mathcal{R} is the residual operator denoted by

$$\mathscr{R}\boldsymbol{u}_{N}^{h} = \mu \Delta \boldsymbol{u}_{N}^{h} + (\lambda + \mu) \nabla (\nabla \cdot \boldsymbol{u}_{N}^{h}) + \omega^{2} \boldsymbol{u}_{N}^{h}.$$

Introduce the weighted norm

It is easy to check that for any $u \in H^1(\Omega)$ we have

$$\min(\mu,\omega^2)\|\boldsymbol{u}\|_{\boldsymbol{H}^1(\Omega)}^2 \leq \|\boldsymbol{u}\|_{\boldsymbol{H}^1(\Omega)}^2 \leq \max(2\lambda+3\mu,\omega^2)\|\boldsymbol{u}\|_{\boldsymbol{H}^1(\Omega)}^2,$$

which implies that the norms $\|\cdot\|_{H^1(\Omega)}$ and $\|\cdot\|_{H^1(\Omega)}$ are equivalent.

Now, let us state the main result of this paper.

THEOREM 4.1. Let \mathbf{u} and \mathbf{u}_N^h be the solutions of the variational problems (2.6) and (3.3), respectively. Let $\boldsymbol{\xi} = \mathbf{u} - \mathbf{u}_N^h$. Then for sufficiently large N, the following a posteriori error estimate holds:

$$\|\boldsymbol{\xi}\|_{\boldsymbol{H}^1(\Omega)} \lesssim \left(\sum_{T \in \mathcal{M}_h} \eta_T^2\right)^{1/2} + N\left(\frac{R'}{R}\right)^N \|\boldsymbol{u}^{\mathrm{inc}}\|_{\boldsymbol{H}^1(\Omega)}.$$

It can be seen from the theorem that the a posteriori error estimate consists of two parts: the first part arises from the finite element discretization error; the second part accounts for the truncation error of the DtN operator, which decreases exponentially with respect to N since R' < R.

Remark 4.2. It is worth pointing out that the constant in the a posteriori error estimate depends implicitly on the frequency ω . It is difficult to obtain the constant with an explicit dependence on the frequency due to the lack of stability estimate in general domains. We refer the reader to [30] for the stability analysis with an explicit dependence on the wavenumber in a spherical shell for Maxwell's equations.

Using (4.1) and the integration by parts, we obtain

$$\begin{aligned} \|\boldsymbol{\xi}\|_{\boldsymbol{H}^{1}(\Omega)}^{2} &= \mu \int_{\Omega} \nabla \boldsymbol{\xi} : \nabla \overline{\boldsymbol{\xi}} d\boldsymbol{x} + (\lambda + \mu) \int_{\Omega} (\nabla \cdot \boldsymbol{\xi}) (\nabla \cdot \overline{\boldsymbol{\xi}}) d\boldsymbol{x} + \omega^{2} \int_{\Omega} \boldsymbol{\xi} \cdot \overline{\boldsymbol{\xi}} d\boldsymbol{x} \\ &= \Re b(\boldsymbol{\xi}, \boldsymbol{\xi}) + 2\omega^{2} \int_{\Omega} \boldsymbol{\xi} \cdot \overline{\boldsymbol{\xi}} d\boldsymbol{x} + \Re \int_{\Gamma_{R}} \mathscr{T} \boldsymbol{\xi} \cdot \overline{\boldsymbol{\xi}} d\boldsymbol{s} \\ &= \Re b(\boldsymbol{\xi}, \boldsymbol{\xi}) + \Re \int_{\Gamma_{R}} (\mathscr{T} - \mathscr{T}_{N}) \boldsymbol{\xi} \cdot \overline{\boldsymbol{\xi}} d\boldsymbol{s} + 2\omega^{2} \int_{\Omega} \boldsymbol{\xi} \cdot \overline{\boldsymbol{\xi}} d\boldsymbol{x} + \Re \int_{\Gamma_{R}} \mathscr{T}_{N} \boldsymbol{\xi} \cdot \overline{\boldsymbol{\xi}} d\boldsymbol{s}. \end{aligned}$$

$$(4.2)$$

To prove Theorem 4.1, it suffices to estimate the four terms given on the right-hand side of (4.2).

The following lemma concerns the trace theorem. The proof is standard and so is omitted for brevity.

Lemma 4.3. For any $u \in H^1(\Omega)$, the following estimates hold:

$$||u||_{H^{1/2}(\Gamma_R)} \lesssim ||u||_{H^1(\Omega)}, \quad ||u||_{H^{1/2}(\Gamma_{R'})} \lesssim ||u||_{H^1(\Omega)}.$$

LEMMA 4.4. Let $\mathbf{u}^s \in \mathbf{H}^1(\Omega)$ be the scattered field corresponding to the solution of the variational problem (2.6). For any $\mathbf{v} \in \mathbf{H}^1(\Omega)$, the following estimate holds:

$$\left| \int_{\Gamma_R} \left(\mathscr{T} - \mathscr{T}_N \right) \boldsymbol{u}^s \cdot \boldsymbol{v} \mathrm{d}s \right| \lesssim N \left(\frac{R'}{R} \right)^N \| \boldsymbol{u}^{\mathrm{inc}} \|_{\boldsymbol{H}^1(\Omega)} \| \boldsymbol{v} \|_{\boldsymbol{H}^1(\Omega)}.$$

Proof. Let ϕ^s and ψ^s be the potentials of the Helmholtz decomposition for the scattered field u^s . It can be verified from (SM4.1)–(SM4.2) that

$$(4.3) \ \phi_n^{sm}(R) = z_n^p \phi_n^{sm}(R'), \ \psi_{2n}^{sm}(R) = z_n^s \psi_{2n}^{sm}(R'), \ \psi_{3n}^{sm}(R) = \left(\frac{R'}{R}\right) z_n^s \psi_{3n}^{sm}(R'),$$

where $z_n^p = h_n^{(1)}(\kappa_p R)/h_n^{(1)}(\kappa_p R')$ and $z_n^s = h_n^{(1)}(\kappa_s R)/h_n^{(1)}(\kappa_s R')$. Substituting (4.3) into (SM4.3) and using (SM4.4) with R being replaced with R', we obtain

$$\boldsymbol{u}_n^{sm}(R) = Q_n \boldsymbol{u}_n^{sm}(R'),$$

where the entries of the matrix Q_n are

$$\begin{split} Q_{n,11} &= \frac{R'}{R\Lambda_n(R')} \left[-n(n+1)z_n^p + z_n^{(1)}(\kappa_p R')(1+z_n^{(1)}(\kappa_s R))z_n^s \right], \\ Q_{n,13} &= \frac{R'}{R\Lambda_n(R')} \sqrt{n(n+1)} \left[(1+z_n^{(1)}(\kappa_s R'))z_n^p - (1+z_n^{(1)}(\kappa_s R))z_n^s \right], \\ Q_{n,31} &= \frac{R'}{R\Lambda_n(R')} \sqrt{n(n+1)} \left[-z_n^{(1)}(\kappa_p R)z_n^p + z_n^{(1)}(\kappa_p R')z_n^s \right], \\ Q_{n,33} &= \frac{R'}{R\Lambda_n(R')} \left[(1+z_n^{(1)}(\kappa_s R'))z_n^{(1)}(\kappa_p R)z_n^p - n(n+1)z_n^s \right], \end{split}$$

and
$$Q_{n,22} = z_n^s$$
, $Q_{n,12} = Q_{n,21} = Q_{n,23} = Q_{n,32} = 0$.

We use the element $Q_{n,11}$ as an example to show the estimate of the matrix Q_n since all the other elements can be similarly estimated. A simple calculation yields

$$Q_{n,11} = \frac{R'}{R\Lambda_n(R')} n(n+1)(z_n^s - z_n^p)$$

$$+ \frac{R'}{R\Lambda_n(R')} \left[z_n^{(1)}(\kappa_p R')(1 + z_n^{(1)}(\kappa_s R)) - n(n+1) \right] z_n^s.$$

It follows from Lemma SM5.5 and (SM5.9)-(SM5.10) that

$$|Q_{n,11}| \lesssim n \left(\frac{R'}{R}\right)^n$$
.

Similarly, we may show that all the other entries of Q_n satisfy

$$|Q_{n,ij}| \lesssim n \left(\frac{R'}{R}\right)^n, \quad i, j = 1, 2, 3.$$

Substituting the estimate of Q_n into (4.4), we have

$$|\boldsymbol{u}_{n}^{sm}(R)| \lesssim n \Big(\frac{R'}{R}\Big)^n |\boldsymbol{u}_{n}^{sm}(R')|.$$

Combining the above estimates with (SM4.6) and using Lemma 4.3 and (2.7) give

$$\left| \int_{\Gamma_R} (\mathcal{T} - \mathcal{T}_N) \, \boldsymbol{u}^s \cdot \boldsymbol{v} \, \mathrm{d}s \right| = \left| \sum_{n > N} \sum_{m = -n}^n M_n \boldsymbol{u}_n^{sm}(R) \cdot \overline{\boldsymbol{v}}_n^m(R) \right|$$

$$= \left| \sum_{n > N} \sum_{m = -n}^n M_n Q_n \boldsymbol{u}_n^{sm}(R') \cdot \overline{\boldsymbol{v}}_n^m(R) \right|$$

$$\lesssim \left| \sum_{n > N} \sum_{m = -n}^n n^2 \left(\frac{R'}{R} \right)^n \boldsymbol{u}_n^{sm}(R') \cdot \overline{\boldsymbol{v}}_n^m(R) \right|$$

$$\lesssim \max_{n > N} \left(n \left(\frac{R'}{R} \right)^n \right) \|\boldsymbol{u}^{\text{inc}}\|_{\boldsymbol{H}^1(\Omega)} \|\boldsymbol{v}\|_{\boldsymbol{H}^1(\Omega)}.$$

The proof is completed by noting that $n\left(R'/R\right)^n$ decreases for sufficiently large n. \square

Based on Lemma 4.4, the estimate of the first two terms in (4.2) is given in the following lemma.

LEMMA 4.5. Let v be any function in $H^1_{\partial D}(\Omega)$; the following estimate holds:

$$\begin{aligned} & \left| b(\boldsymbol{\xi}, \boldsymbol{v}) + \int_{\Gamma_R} \left(\mathscr{T} - \mathscr{T}_N \right) \boldsymbol{\xi} \cdot \overline{\boldsymbol{v}} \mathrm{d}s \right| \\ & \lesssim \left(\left(\sum_{K \in \mathcal{M}_h} \eta_K^2 \right)^{1/2} + N \left(\frac{\hat{R}}{R} \right)^N \| \boldsymbol{u}^{\mathrm{inc}} \|_{\boldsymbol{H}^1(\Omega)} \right) \| \boldsymbol{v} \|_{\boldsymbol{H}^1(\Omega)}. \end{aligned}$$

Proof. For any function \boldsymbol{v} in $\boldsymbol{H}_{\partial D}^{1}(\Omega)$ and \boldsymbol{v}^{h} in $\boldsymbol{V}_{h,\partial D}$, we have

$$\begin{split} b(\boldsymbol{\xi}, \boldsymbol{v}) + \int_{\Gamma_R} \left(\mathscr{T} - \mathscr{T}_N \right) \boldsymbol{\xi} \cdot \overline{\boldsymbol{v}} \mathrm{d}s \\ &= b(\boldsymbol{u}, \boldsymbol{v}) - b_N^h(\boldsymbol{u}_N^h, \boldsymbol{v}^h) + b_N^h(\boldsymbol{u}_N^h, \boldsymbol{v}^h) - b(\boldsymbol{u}_h^h, \boldsymbol{v}) + \int_{\Gamma_R} (\mathscr{T} - \mathscr{T}_N) \boldsymbol{\xi} \cdot \overline{\boldsymbol{v}} \mathrm{d}s \\ &= \int_{\Gamma_R} \boldsymbol{g}_N \cdot \left(\overline{\boldsymbol{v}} - \overline{\boldsymbol{v}^h} \right) \mathrm{d}s - b_N^h(\boldsymbol{u}_N^h, \boldsymbol{v} - \boldsymbol{v}^h) \\ &+ \int_{\Gamma_R} (\boldsymbol{g} - \boldsymbol{g}_N) \cdot \overline{\boldsymbol{v}} \mathrm{d}s + \int_{\Gamma_R} (\mathscr{T} - \mathscr{T}_N) \boldsymbol{u} \cdot \overline{\boldsymbol{v}} \mathrm{d}s. \end{split}$$

Using integration by parts yields

$$\begin{split} &-b_{N}(\boldsymbol{u}_{N}^{h},\boldsymbol{v}-\boldsymbol{v}^{h})+\left(\boldsymbol{g}_{N},\boldsymbol{v}-\boldsymbol{v}^{h}\right)\\ &=-\sum_{K\in\mathcal{M}_{h}}\left\{\mu\int_{K}\nabla\boldsymbol{u}_{N}^{h}:\nabla(\overline{\boldsymbol{v}}-\overline{\boldsymbol{v}^{h}})\mathrm{d}\boldsymbol{x}+(\lambda+\mu)\int_{K}\left(\nabla\cdot\boldsymbol{u}_{N}^{h}\right)\nabla\cdot\left(\overline{\boldsymbol{v}}-\overline{\boldsymbol{v}^{h}}\right)\mathrm{d}\boldsymbol{x}\right\}\\ &-\sum_{K\in\mathcal{M}_{h}}\left\{-\omega^{2}\int_{K}\boldsymbol{u}_{N}^{h}\cdot\left(\overline{\boldsymbol{v}}-\overline{\boldsymbol{v}^{h}}\right)\mathrm{d}\boldsymbol{x}-\int_{\Gamma_{R}\cap\partial K}\left(\mathscr{T}_{N}\boldsymbol{u}_{N}^{h}+\boldsymbol{g}_{N}\right)\cdot\left(\overline{\boldsymbol{v}}-\overline{\boldsymbol{v}^{h}}\right)\mathrm{d}\boldsymbol{s}\right\}\\ &=\sum_{K\in\mathcal{M}_{h}}\left\{-\int_{\partial K}\left[\mu\nabla\boldsymbol{u}_{N}^{h}\cdot\boldsymbol{\nu}+(\lambda+\mu)(\nabla\cdot\boldsymbol{u}_{N}^{h})\boldsymbol{\nu}\right]\cdot\left(\overline{\boldsymbol{v}}-\overline{\boldsymbol{v}^{h}}\right)\mathrm{d}\boldsymbol{x}\right.\\ &+\int_{\Gamma_{R}\cap\partial K}\left(\mathscr{T}_{N}\boldsymbol{u}_{N}^{h}+\boldsymbol{g}_{N}\right)\cdot\left(\overline{\boldsymbol{v}}-\overline{\boldsymbol{v}^{h}}\right)\mathrm{d}\boldsymbol{s}\right\}\\ &+\sum_{K\in\mathcal{M}_{h}}\int_{K}\left[\mu\Delta\boldsymbol{u}_{N}^{h}+(\lambda+\mu)\nabla\nabla\cdot\boldsymbol{u}_{N}^{h}+\omega^{2}\boldsymbol{u}_{N}^{h}\right]\cdot\left(\overline{\boldsymbol{v}}-\overline{\boldsymbol{v}^{h}}\right)\mathrm{d}\boldsymbol{x}\\ &=\sum_{K\in\mathcal{M}_{h}}\left[\int_{K}\mathscr{R}\boldsymbol{u}_{N}^{h}\cdot\left(\overline{\boldsymbol{v}}-\overline{\boldsymbol{v}^{h}}\right)\mathrm{d}\boldsymbol{x}+\sum_{e\in\partial K}\frac{1}{2}\int_{e}J_{e}\cdot\left(\overline{\boldsymbol{v}}-\overline{\boldsymbol{v}^{h}}\right)\mathrm{d}\boldsymbol{s}\right]. \end{split}$$

By the definitions of g and g_N , we get

$$\begin{split} \int_{\Gamma_R} \left(\boldsymbol{g} - \boldsymbol{g}_N^h \right) \cdot \overline{\boldsymbol{v}} \mathrm{d}s &= \int_{\Gamma_R} \left[\left(\mathscr{B} \boldsymbol{u}^{\mathrm{inc}} - \mathscr{T} \boldsymbol{u}^{\mathrm{inc}} \right) - \left(\mathscr{B} \boldsymbol{u}^{\mathrm{inc}} - \mathscr{T}_N \boldsymbol{u}^{\mathrm{inc}} \right) \right] \cdot \boldsymbol{v} \mathrm{d}s \\ &= \int_{\Gamma_R} \left(\mathscr{T}_N - \mathscr{T} \right) \boldsymbol{u}^{\mathrm{inc}} \cdot \boldsymbol{v} \mathrm{d}s. \end{split}$$

It follows from Lemma 4.4 that

$$\begin{split} & \left| \left(\boldsymbol{g} - \boldsymbol{g}_N^h, \boldsymbol{v} \right)_{\partial B_R} + \left(\left(\mathscr{T} - \mathscr{T}_N \right) \boldsymbol{u}, \boldsymbol{v} \right)_{\partial B_R} \right| \\ & = \left| \int_{\Gamma_R} \left(\mathscr{T} - \mathscr{T}_N \right) \boldsymbol{u}^s \cdot \boldsymbol{v} \mathrm{d}s \right| \lesssim N \bigg(\frac{\hat{R}}{R} \bigg)^N \| \boldsymbol{u}^{\mathrm{inc}} \|_{\boldsymbol{H}^1(\Omega)} \| \boldsymbol{v} \|_{\boldsymbol{H}^1(\Omega)}. \end{split}$$

The proof is completed by combining the above estimates.

It is proved in [27] that the matrix $\hat{M}_n = -\frac{1}{2} (M_n + M_n^*)$ is positive definite for sufficiently large n, where the star denotes the complex transpose. The following result can be obtained easily by following the proof of [28, Lemma 4.6].

Lemma 4.6. For any $\delta > 0$, there exists a positive constant $C(\delta)$ independent of N such that

$$\int_{\Gamma_R} \mathscr{T}_N \boldsymbol{\xi} \cdot \overline{\boldsymbol{\xi}} ds \le C(\delta) \|\boldsymbol{\xi}\|_{\boldsymbol{L}^2(B_R \setminus B_{R'})}^2 + \left(\frac{R}{R'}\right) \delta \|\boldsymbol{\xi}\|_{\boldsymbol{H}^1(B_R \setminus B_{R'})}^2.$$

To estimate the third term of (4.2), we introduce the dual problem

$$b(\boldsymbol{v}, \boldsymbol{p}) = \int_{\Omega} \boldsymbol{v} \cdot \overline{\boldsymbol{\xi}} d\boldsymbol{x} \quad \forall \, \boldsymbol{v} \in \boldsymbol{H}^{1}_{\partial D}(\Omega).$$

It is easy to verify that p satisfies the boundary value problem

(4.6)
$$\begin{cases} \mu \Delta \boldsymbol{p} + (\lambda + \mu) \nabla \nabla \cdot \boldsymbol{p} + \omega^2 \boldsymbol{p} = -\boldsymbol{\xi} & \text{in } \Omega, \\ \boldsymbol{p} = 0 & \text{on } \partial D, \\ \mathscr{D} \boldsymbol{p} = \mathscr{T}^* \boldsymbol{p} & \text{on } \Gamma_R, \end{cases}$$

where \mathscr{T}^* is the adjoint operator to the DtN operator \mathscr{T} . Letting $\boldsymbol{v} = \boldsymbol{\xi}$ in (4.5) leads to

$$(4.7) \|\boldsymbol{\xi}\|_{\boldsymbol{L}^{2}(\Omega)}^{2} = b(\boldsymbol{\xi}, \boldsymbol{p}) + \int_{\Gamma_{R}} (\mathscr{T} - \mathscr{T}_{N}) \boldsymbol{\xi} \cdot \overline{\boldsymbol{p}} ds - \int_{\Gamma_{R}} (\mathscr{T} - \mathscr{T}_{N}) \boldsymbol{\xi} \cdot \overline{\boldsymbol{p}} ds.$$

The first two terms of (4.7) can be estimated in the same way as that of Lemma 4.5. Thus it suffices to estimate the third term of (4.7). Next we deduce the solution of the dual problem (4.5) which is crucial for the estimate.

Consider the system

(4.8)
$$\begin{cases} \nabla \zeta + \nabla \times \mathbf{Z} = \boldsymbol{\xi}, \quad \nabla \cdot \mathbf{Z} = 0 & \text{in } B_R \setminus \overline{B_{R'}}, \\ \zeta(R) = 0, \quad \mathbf{Z}(R) = 0 & \text{on } \Gamma_R. \end{cases}$$

By a straightforward calculation, the Fourier coefficients for the solution of (4.8) are given by

$$\zeta_{n}^{m}(\rho) = \frac{1}{2n+1} \int_{\rho}^{R} \left[-nc_{2} - (n+1)c_{4} \right] \xi_{3n}^{m}(\tau)$$

$$(4.9) \qquad \qquad -\sqrt{n(n+1)}(c_{2} - c_{4}) \xi_{1n}^{m}(\tau) d\tau,$$

$$Z_{1n}^{m}(\rho) = \frac{1}{2n+1} \int_{\rho}^{R} \left[-nc_{1} - (n+1)c_{3} \right] \xi_{2n}^{m}(\tau) d\tau,$$

$$Z_{2n}^{m}(\rho) = \frac{1}{2n+1} \int_{\rho}^{R} \sqrt{n(n+1)}(c_{2} - c_{4}) \xi_{3n}^{m}(\tau) + \left[(n+1)c_{2} + nc_{4} \right] \xi_{1n}^{m}(\tau) d\tau,$$

$$(4.11)$$

(4.12)
$$Z_{3n}^m(\rho) = \frac{1}{2n+1} \int_{\rho}^{R} \sqrt{n(n+1)} (c_1 - c_3) \xi_{2n}^m(\tau) d\tau,$$

where

$$c_1 = \left(\frac{\rho}{\tau}\right)^{-n-2}, \quad c_2 = \left(\frac{\rho}{\tau}\right)^{-n-1}, \quad c_3 = \left(\frac{\rho}{\tau}\right)^{n-1}, \quad c_4 = \left(\frac{\rho}{\tau}\right)^n.$$

Consider the following boundary value problem:

$$(4.13) \begin{cases} \Delta g + \kappa_p^2 g = -\frac{1}{\lambda + 2\mu} \zeta, & -\nabla \times (\nabla \times \boldsymbol{q}) + \kappa_s^2 \boldsymbol{q} = -\frac{1}{\mu} \boldsymbol{Z} & \text{in } B_R \setminus B_{R'}, \\ \nabla \cdot \boldsymbol{q} = \nabla \cdot \boldsymbol{Z} = 0 & \text{in } B_R \setminus B_{R'}, \\ \partial_{\rho} g = \mathscr{T}_1^* g, & (\nabla \times \boldsymbol{q}) \times \boldsymbol{e}_{\rho} = -\mathrm{i} \kappa_s \mathscr{T}_2^* \boldsymbol{q}_{\Gamma_R} & \text{on } \Gamma_R, \\ g = g, & \boldsymbol{q} = \boldsymbol{q} & \text{on } \Gamma_{R'}, \end{cases}$$

where \mathscr{T}_1^* and \mathscr{T}_2^* are the adjoint operators to the DtN operators \mathscr{T}_1 (cf. (SM4.7)) and \mathscr{T}_2 (cf. (SM4.8)), respectively, and $\mathbf{q}_{\Gamma_R} = -\mathbf{e}_{\rho} \times (\mathbf{e}_{\rho} \times \mathbf{q})$ is the tangential component of \mathbf{q} on Γ_R .

LEMMA 4.7. If (ζ, \mathbf{Z}) and (g, \mathbf{q}) are the solutions of the systems (4.8) and (4.13), respectively, then $\mathbf{p} = \nabla g + \nabla \times \mathbf{q}$ is the solution of the dual problem (4.6) in $B_R \setminus \overline{B_{R'}}$.

Proof. Letting $\boldsymbol{p} = \nabla g + \nabla \times \boldsymbol{q}$ and substituting it into the elastic wave equation, we get

$$\mu\Delta (\nabla g + \nabla \times \mathbf{q}) + (\lambda + \mu)\nabla\nabla \cdot (\nabla g + \nabla \times \mathbf{q}) + \omega^2 (\nabla g + \nabla \times \mathbf{q})$$

$$= \nabla ((\lambda + 2\mu)\Delta g + \omega^2 g) + \nabla \times (-\mu\nabla \times \nabla \times \mathbf{q} + \mu\nabla\nabla \cdot \mathbf{q} + \omega^2 \mathbf{q})$$

$$= -\nabla \zeta - \nabla \times \mathbf{Z} = -\boldsymbol{\xi},$$

which shows that p satisfies the elastic wave equation in (4.6). The rest of the proof is to show that p satisfies the boundary condition $\mathcal{D}p = \mathcal{T}^*p$ on Γ_R .

It follows from (SM2.1)-(SM2.2) that

$$p = \nabla g + \nabla \times q$$

$$= \sum_{n \in \mathbb{N}} \sum_{|m| \le n} \left[\frac{\sqrt{n(n+1)}}{\rho} g_n^m(\rho) - \frac{1}{\rho} q_{2n}^m(\rho) - q_{2n}^{m'}(\rho) \right] \boldsymbol{U}_n^m$$

$$+ \left[\frac{1}{\rho} q_{1n}^m(\rho) + q_{1n}^{m'}(\rho) - \frac{\sqrt{n(n+1)}}{\rho} q_{3n}^m(\rho) \right] \boldsymbol{V}_n^m$$

$$+ \left[g_n^{m'}(\rho) - \frac{\sqrt{n(n+1)}}{\rho} q_{2n}^m(\rho) \right] \boldsymbol{X}_n^m \boldsymbol{e}_{\rho}.$$

$$(4.14)$$

Let $v_n^m(\rho) = \rho q_{3n}^m(\rho)$. Since $\nabla \cdot \mathbf{q} = 0$, we have from (SM2.3) that

$$\begin{split} q_{1n}^m(\rho) &= \frac{1}{\sqrt{n(n+1)}} \frac{1}{\rho} \left(v_n^m(\rho) + \rho v_n^{m'}(\rho) \right), \\ q_{1n}^{m'}(\rho) &= \frac{1}{\sqrt{n(n+1)}} \left(-\frac{1}{\rho^2} v_n^m(\rho) + \frac{1}{\rho} v_n^{m'}(\rho) + v_n^{m''}(\rho) \right). \end{split}$$

It follows from Lemma SM6.3 that

$$\frac{1}{\rho}q_{1n}^{m}(\rho) + q_{1n}^{m'}(\rho) - \frac{\sqrt{n(n+1)}}{\rho}q_{3n}^{m}(\rho)
= \frac{1}{\sqrt{n(n+1)}} \left(v_{n}^{m''}(\rho) + \frac{2}{\rho}v_{n}^{m'}(\rho) - \frac{n(n+1)}{\rho^{2}}v_{n}^{m}(\rho) \right)
= -\frac{1}{\sqrt{n(n+1)}} \left(\beta_{n}^{m}(\rho) + \kappa_{s}^{2}v_{n}^{m}(\rho) \right).$$
(4.15)

Substituting (4.15) into (4.14) and taking derivative of p, we obtain

$$p'(\rho) = \sum_{n \in \mathbb{N}} \sum_{|m| \le n} \left[\sqrt{n(n+1)} \frac{\partial}{\partial \rho} \left(\frac{1}{\rho} g_n^m(\rho) \right) - \frac{\partial}{\partial \rho} \left(\frac{1}{\rho} q_{2n}^m(\rho) \right) - q_{2n}^{m''}(\rho) \right] \boldsymbol{U}_n^m$$

$$- \frac{1}{\sqrt{n(n+1)}} \left[\beta_n^{m'}(\rho) + \kappa_s^2 v_n^{m'}(\rho) \right] \boldsymbol{V}_n^m$$

$$+ \left[g_n^{m''}(\rho) - \sqrt{n(n+1)} \frac{\partial}{\partial \rho} \left(\frac{1}{\rho} q_{2n}^m(\rho) \right) \right] \boldsymbol{X}_n^m \boldsymbol{e}_{\rho}.$$

$$(4.16)$$

A simple calculation yields

(4.17)
$$\nabla \cdot \boldsymbol{p} = \Delta g = -\frac{1}{\lambda + 2\mu} \zeta - \kappa_p^2 g.$$

Substituting (4.16)–(4.17) into the boundary operator \mathcal{D} , we have

$$\mathscr{D}\boldsymbol{p} = \mu \partial_{\rho}\boldsymbol{p} + (\lambda + \mu)(\nabla \cdot \boldsymbol{p})\boldsymbol{e}_{\rho}
= \sum_{n \in \mathbb{N}} \sum_{|m| \le n} \left\{ \left[\mu g_{n}^{m''}(\rho) - (\lambda + \mu) \kappa_{p}^{2} g_{n}^{m}(\rho) \right] X_{n}^{m} \boldsymbol{e}_{\rho} \right.
+ \mu \sqrt{n(n+1)} \frac{\partial}{\partial \rho} \left(\frac{1}{\rho} g_{n}^{m}(\rho) \right) \boldsymbol{U}_{n}^{m} \right\}
+ \mu \sum_{n \in \mathbb{N}} \sum_{|m| \le n} \left\{ -\left[\frac{\partial}{\partial \rho} \left(\frac{1}{\rho} q_{2n}^{m}(\rho) \right) + q_{2n}^{m''}(\rho) \right] \boldsymbol{U}_{n}^{m} \right.
- \sqrt{n(n+1)} \frac{\partial}{\partial \rho} \left(\frac{1}{\rho} q_{2n}^{m}(\rho) \right) X_{n}^{m} \boldsymbol{e}_{\rho} \right.
- \frac{1}{\sqrt{n(n+1)}} \left[\beta_{n}^{m'}(\rho) + \kappa_{s}^{2} v_{n}^{m'}(\rho) \right] \boldsymbol{V}_{n}^{m} \right\} - \left(\frac{\lambda + \mu}{\lambda + 2\mu} \right) \zeta \boldsymbol{e}_{\rho}$$

$$(4.18) \qquad =: I_{1} + I_{2} + I_{3},$$

where I_1 , I_2 , and I_3 account for the summation of g_n^m , q_{2n}^m , and q_{3n}^m , respectively. It follows from (SM2.4) that

$$\Delta g + \kappa_p^2 g = -\frac{1}{\lambda + 2\mu} \zeta,$$

which gives

$$\sum_{n \in \mathbb{N}} \sum_{|m| \le n} \left[g_n^{m''}(\rho) + \frac{2}{\rho} g_n^{m'}(\rho) - \frac{n(n+1)}{\rho^2} g_n^m(\rho) + \kappa_p^2 g_n^m \right] X_n^m + \frac{1}{\lambda + 2\mu} \zeta = 0.$$

Substituting the above equation into I_1 and replacing the second order derivative give

$$\begin{split} I_1 &= \sum_{n \in \mathbb{N}} \sum_{|m| \le n} \left\{ \left[\mu g_n^{m''}(\rho) - (\lambda + \mu) \kappa_p^2 g_n^m(\rho) \right] X_n^m \boldsymbol{e}_\rho \right. \\ &+ \mu \sqrt{n(n+1)} \frac{\partial}{\partial \rho} \left(\frac{1}{\rho} g_n^m(\rho) \right) \boldsymbol{U}_n^m \right\} \\ &= \sum_{n \in \mathbb{N}} \sum_{|m| \le n} \left\{ \left[-\mu \frac{2}{\rho} g_n^{m'}(\rho) + \mu \frac{n(n+1)}{\rho^2} g_n^m(\rho) - \omega^2 g_n^m(\rho) \right] X_n^m \boldsymbol{e}_\rho \right. \\ &+ \mu \sqrt{n(n+1)} \left[\frac{1}{\rho} g_n^{m'}(\rho) - \frac{1}{\rho^2} g_n^m(\rho) \right] \boldsymbol{U}_n^m \right\}. \end{split}$$

Replacing the first order derivative by the TBC

$$g_n^{m'}(R) = \frac{z_n^{(2)}(\kappa_p R)}{R} g_n^m(R).$$

we have from a straightforward computation that

$$I_{1}(R) = \frac{1}{R^{2}} \sum_{n \in \mathbb{N}} \sum_{|m| \le n} \left\{ \left[-2\mu z_{n}^{(2)}(\kappa_{p}R) + n(n+1)\mu - \omega^{2}R^{2} \right] g_{n}^{m}(R) X_{n}^{m} \boldsymbol{e}_{\rho} + \mu \sqrt{n(n+1)} \left[z_{n}^{(2)}(\kappa_{p}R) - 1 \right] g_{n}^{m}(R) \boldsymbol{U}_{n}^{m} \right\}.$$

Using (4.13) and (SM2.5), we get

$$-\frac{1}{\rho}\frac{\partial^2}{\partial\rho^2}\left(\rho q_{2n}^m(\rho)\right)+\frac{n(n+1)}{\rho^2}q_{2n}^m(\rho)-\kappa_s^2q_{2n}^m(\rho)=\frac{1}{\mu}Z_{2n}^m(\rho),$$

which implies that

$$q_{2n}^{m''}(\rho) = -\frac{2}{\rho}q_{2n}^{m'}(\rho) + \frac{n(n+1)}{\rho^2}q_{2n}^m(\rho) - \kappa_s^2q_{2n}^m(\rho) - \frac{1}{\mu}Z_{2n}^m(\rho).$$

Substituting the above equation into I_2 and replacing the second derivative leads to

$$\begin{split} I_{2} &= \mu \sum_{n \in \mathbb{N}} \sum_{|m| \le n} \left\{ -\left[q_{2n}^{m''}(\rho) + \left(-\frac{1}{\rho^{2}} q_{2n}^{m}(\rho) + \frac{1}{\rho} q_{2n}^{m'}(\rho) \right) \right] \boldsymbol{U}_{n}^{m} \right. \\ &- \sqrt{n(n+1)} \left(-\frac{1}{\rho^{2}} q_{2n}^{m}(\rho) + \frac{1}{\rho} q_{2n}^{m'}(\rho) \right) \boldsymbol{X}_{n}^{m} \boldsymbol{e}_{\rho} \right\} \\ &= \mu \sum_{n \in \mathbb{N}} \sum_{|m| \le n} \left\{ \left[\frac{2}{\rho} q_{2n}^{m'}(\rho) - \frac{n(n+1)}{\rho^{2}} q_{2n}^{m}(\rho) + \kappa_{s}^{2} q_{2n}^{m}(\rho) + \frac{1}{\mu} Z_{2n}^{m}(\rho) \right. \\ &+ \frac{1}{\rho^{2}} q_{2n}^{m}(\rho) - \frac{1}{\rho} q_{2n}^{m'}(\rho) \right] \boldsymbol{U}_{n}^{m} - \sqrt{n(n+1)} \left(-\frac{1}{\rho^{2}} q_{2n}^{m}(\rho) + \frac{1}{\rho} q_{2n}^{m'}(\rho) \right) \boldsymbol{X}_{n}^{m} \boldsymbol{e}_{\rho} \right\} \\ &= \mu \sum_{n \in \mathbb{N}} \sum_{|m| \le n} \left\{ \left[\frac{1}{\rho} q_{2n}^{m'}(\rho) + \left(\kappa_{s}^{2} + \frac{1}{\rho^{2}} - \frac{n(n+1)}{\rho^{2}} \right) q_{2n}^{m}(\rho) \right] \boldsymbol{U}_{n}^{m} \\ &- \sqrt{n(n+1)} \left[\frac{1}{\rho} q_{2n}^{m'}(\rho) - \frac{1}{\rho^{2}} q_{2n}^{m}(\rho) \right] \boldsymbol{X}_{n}^{m} \boldsymbol{e}_{\rho} \right\}. \end{split}$$

Note that the terms Z_{1n}^m and ζ vanish on Γ_R . Substituting the TBC back into I_2 and eliminating the first order terms, we deduce

$$I_{2}(R) = \frac{\mu}{R^{2}} \sum_{n \in \mathbb{N}} \sum_{|m| \le n} \left\{ \left[z_{n}^{(2)}(\kappa_{s}R) + \kappa_{s}^{2}R^{2} + 1 - n(n+1) \right] q_{2n}^{m}(R) \boldsymbol{U}_{n}^{m} - \sqrt{n(n+1)} \left[z_{n}^{(2)}(\kappa_{s}R) - 1 \right] q_{2n}^{m}(R) X_{n}^{m} \boldsymbol{e}_{\rho} \right\}.$$

By (4.12), we have $\beta_n^{m'}(R) = 0$. It follows from Lemma SM6.3 that

$$I_{3}(R) = -\mu \sum_{n \in \mathbb{N}} \sum_{|m| \le n} \frac{1}{\sqrt{n(n+1)}} \left[\beta_{n}^{m'}(R) + \kappa_{s}^{2} v_{n}^{m'}(R) \right] \boldsymbol{V}_{n}^{m}$$
$$= -\sum_{n \in \mathbb{N}} \sum_{|m| \le n} \frac{\mu \kappa_{s}^{2}}{\sqrt{n(n+1)}} z_{n}^{(2)}(\kappa_{s} R) q_{3n}^{m}(R) \boldsymbol{V}_{n}^{m}.$$

Substituting I_1 , I_2 , and I_3 into (4.18), we get

$$\mathscr{D}p = I_{1}(R) + I_{2}(R) + I_{3}(R)
= \frac{1}{R^{2}} \sum_{n \in \mathbb{N}} \sum_{|m| \leq n} \left\{ \left[-2\mu z_{n}^{(2)}(\kappa_{p}R) + n(n+1)\mu - \omega^{2}R^{2} \right] g_{n}^{m}(R) X_{n}^{m} \boldsymbol{e}_{\rho} \right.
+ \mu \sqrt{n(n+1)} \left[z_{n}^{(2)}(\kappa_{p}R) - 1 \right] g_{n}^{m}(R) \boldsymbol{U}_{n}^{m} \right\}
+ \frac{\mu}{R^{2}} \sum_{n \in \mathbb{N}} \sum_{|m| \leq n} \left\{ \left[z_{n}^{(2)}(\kappa_{s}R) + \kappa_{s}^{2}R^{2} + 1 - n(n+1) \right] q_{2n}^{m}(R) \boldsymbol{U}_{n}^{m} \right.
(4.19) - \sqrt{n(n+1)} \left[z_{n}^{(2)}(\kappa_{s}R) - 1 \right] q_{2n}^{m}(R) X_{n}^{m} \boldsymbol{e}_{\rho} - \frac{z_{n}^{(2)}(\kappa_{s}R) \kappa_{s}^{2}R^{2}}{\sqrt{n(n+1)}} q_{3n}^{m}(R) \boldsymbol{V}_{n}^{m} \right\}.$$

Note that (4.19) is the complex conjugate of (16) in [27]. Using the fact that the TBCs of g and q are the complex conjugate of the original TBCs, we deduce $\mathscr{D}p = \mathscr{T}^*p$ on Γ_R and complete the proof.

Lemma 4.8. Let

$$\boldsymbol{p}(\rho,\theta,\varphi) = \sum_{n=0}^{\infty} \sum_{m=-n}^{n} p_{1n}^{m}(\rho) \boldsymbol{U}_{n}^{m}(\theta,\varphi) + p_{2n}^{m}(\rho) \boldsymbol{V}_{n}^{m}(\theta,\varphi) + p_{3n}^{m}(\rho) X_{n}^{m}(\theta,\varphi) \boldsymbol{e}_{\rho}$$

be the solution of (4.6) in $B_R \setminus \overline{B_{R'}}$. Then the following estimate holds:

$$|p_{jn}^m(R)| \lesssim n \left(\frac{R'}{R}\right)^n \sum_{i=1}^3 |p_{in}^m(R')| + \frac{1}{n} \|\boldsymbol{\xi}\|_{L^{\infty}([R',R])}, \quad j = 1, 2, 3.$$

Proof. It follows from (4.14), (SM6.2), and (SM6.5) that

$$\begin{split} p_{1n}^m(R) &= \frac{\sqrt{n(n+1)}}{R} g_n^m(R) - \frac{1}{R} q_{2n}^m(R) - \frac{1}{R} z_n^{(2)}(\kappa_s R) q_{2n}^m(R) \\ &= \frac{\sqrt{n(n+1)}}{R} \left[S_n^p(R) g_n^m(R') + \frac{\mathrm{i} \kappa_p}{2} \int_{R'}^R t^2 S_n^p(R) W_n^p(R', t) \hat{\zeta}_n^m(t) \mathrm{d}t \right] \\ &- \frac{1}{R} \left[1 + z_n^{(2)}(\kappa_s R) \right] \left[S_n^s(R) q_{2n}^m(R') + \frac{\mathrm{i} \kappa_s}{2} \int_{R'}^R t^2 S_n^s(R) W_n^s(R', t) \hat{Z}_{2n}^m(t) \mathrm{d}t \right]. \end{split}$$

Using (4.14) and (SM6.7) yields

$$\begin{split} p^m_{2n}(R) &= -\frac{1}{\sqrt{n(n+1)}} \kappa_s^2 R q^m_{3n}(R) \\ &= -\frac{1}{\sqrt{n(n+1)}} \kappa_s^2 R \left[\frac{R'}{R} S^s_n(R) q^m_{3n}(R') + \frac{\mathrm{i} \kappa_s}{2R} \int_{R'}^R t^3 S^s_n(R) W^s_n(R',t) \hat{Z}^m_{3n}(t) \mathrm{d}t \right] \\ &= -\frac{1}{\sqrt{n(n+1)}} \kappa_s^2 \left[R' S^s_n(R) q^m_{3n}(R') + \frac{\mathrm{i} \kappa_s}{2} \int_{R'}^R t^3 S^s_n(R) W^s_n(R',t) \hat{Z}^m_{3n}(t) \mathrm{d}t \right]. \end{split}$$

We have from (4.14), (SM6.2), and (SM6.5) that

$$\begin{split} p^m_{3n}(R) &= \frac{1}{R} z_n^{(2)}(\kappa_p R) g_n^m(R) - \frac{\sqrt{n(n+1)}}{R} q_{2n}^m(R) \\ &= \frac{1}{R} z_n^{(2)}(\kappa_p R) \left[S_n^p(R) g_n^m(R') + \frac{\mathrm{i} \kappa_p}{2} \int_{R'}^R t^2 S_n^p(R) W_n^p(R',t) \hat{\zeta}_n^m(t) \mathrm{d}t \right] \\ &- \frac{\sqrt{n(n+1)}}{R} \left[S_n^s(R) q_{2n}^m(R') + \frac{\mathrm{i} \kappa_s}{2} \int_{R'}^R t^2 S_n^s(R) W_n^s(R',t) \hat{Z}_{2n}^m(t) \mathrm{d}t \right]. \end{split}$$

Denote a diagonal matrix by

$$M_{\text{diag}} = \text{diag}\left(\frac{h_n^{(1)}(\kappa_p R)}{h_n^{(1)'}(\kappa_p R')}, \quad \frac{h_n^{(1)}(\kappa_s R)}{h_n^{(1)'}(\kappa_s R')}, \quad \frac{h_n^{(1)}(\kappa_s R)}{h_n^{(1)'}(\kappa_s R')}\right).$$

It is easy to check that

$$(p_{1n}^{m}(R), p_{2n}^{m}(R), p_{3n}^{m}(R))^{\top} = \overline{K_n(R)} \overline{M_{\text{diag}}} \left(g_n^{m}(R'), q_{2n}^{m}(R'), q_{3n}^{m}(R') \right)^{\top} + \overline{K_n(R)} \overline{M_{\text{diag}}} \left(b_{1n}^{m}, b_{2n}^{m}, b_{3n}^{m} \right)^{\top},$$

$$(4.20)$$

where

$$\begin{aligned} \boldsymbol{b}_{n}^{m} &= (b_{1n}^{m}, b_{2n}^{m}, b_{3n}^{m})^{\top} = \left(\frac{\mathrm{i}\kappa_{p}}{2} \int_{R'}^{R} t^{2} W_{n}^{p}(R', t) \hat{\zeta}_{n}^{m}(t) \mathrm{d}t, \ \frac{\mathrm{i}\kappa_{s}}{2} \int_{R'}^{R} t^{2} W_{n}^{s}(R', t) \hat{Z}_{2n}^{m}(t) \mathrm{d}t, \\ \frac{\mathrm{i}\kappa_{s}}{2RR'} \int_{R'}^{R} t^{3} W_{n}^{s}(R', t) \hat{Z}_{3n}^{m}(t) \mathrm{d}t \right)^{\top}. \end{aligned}$$

The next step is to estimate p at $\rho = R'$. By (4.14) and (SM6.8), we have

$$p_{1n}^{m}(R') = \frac{\sqrt{n(n+1)}}{R'} g_{n}^{m}(R') - \frac{1}{R'} q_{2n}^{m}(R') - q_{2n}^{m'}(R')$$

$$= \frac{\sqrt{n(n+1)}}{R'} g_{n}^{m}(R') - \frac{1}{R'} q_{2n}^{m}(R') - \frac{1}{R'} z_{n}^{(2)}(\kappa_{s}R') q_{2n}^{m}(R')$$

$$- \frac{2\kappa_{s}}{\pi R'} \int_{R'}^{R} t^{2} S_{n}^{s}(t) \hat{Z}_{2n}^{m}(t) dt$$

$$= \frac{\sqrt{n(n+1)}}{R'} g_{n}^{m}(R') - \left[1 + z_{n}^{(2)}(\kappa_{s}R')\right] \frac{1}{R'} q_{2n}^{m}(R')$$

$$- \frac{2\kappa_{s}}{\pi R'} \int_{R'}^{R} t^{2} S_{n}^{s}(t) \hat{Z}_{2n}^{m}(t) dt.$$

$$(4.21)$$

A simple calculation from (4.14)–(4.15) yields

(4.22)
$$p_{2n}^m(R') = -\frac{1}{\sqrt{n(n+1)}} \left[\kappa_s^2 R' q_{3n}^m(R') + R' \hat{Z}_{3n}^m(R') \right].$$

It follows from (4.14) and (SM6.3) that

$$p_{3n}^{m}(R') = g_{n}^{m'}(R') - \frac{\sqrt{n(n+1)}}{R'} q_{2n}^{m}(R')$$

$$(4.23) \qquad = \frac{1}{R'} z_{n}^{(2)}(\kappa_{p}R') g_{n}^{m}(R') + \frac{2\kappa_{p}}{\pi R'} \int_{R'}^{R} t^{2} S_{n}^{p}(t) \hat{\zeta}_{n}^{m}(t) dt - \frac{\sqrt{n(n+1)}}{R'} q_{2n}^{m}(R').$$

We get from (4.21)-(4.23) that

$$(p_{1n}^{m}(R'), p_{2n}^{m}(R'), p_{3n}^{m}(R'))^{\top} = \overline{K_n(R')} (g_n^{m}(R'), q_{2n}^{m}(R'), q_{3n}^{m}(R'))^{\top} + (d_{1n}^{m}, d_{2n}^{m}, d_{3n}^{m})^{\top},$$

$$(4.24)$$

where

$$\mathbf{d}_{n}^{m} = (d_{1n}^{m}, d_{2n}^{m}, d_{3n}^{m})^{\top} = \left(-\frac{2\kappa_{s}}{\pi R'} \int_{R'}^{R} t^{2} S_{n}^{s}(t) \hat{Z}_{2n}^{m}(t) dt, -\frac{1}{\sqrt{n(n+1)}} R' \hat{Z}_{3n}^{m}(R'), \frac{2\kappa_{p}}{\pi R'} \int_{R'}^{R} t^{2} S_{n}^{p}(t) \hat{\zeta}_{n}^{m}(t) dt\right)^{\top}.$$

Substituting (4.24) into (4.20) and using the definition (4.4), we obtain

$$(4.26) p_n^m(R) = \overline{Q_n} \, p_n^m(R') - \overline{Q_n} \, d_n^m + \overline{K_n(R)} \, \overline{M_{\text{diag}}} \, b_n^m.$$

By (4.9), it can be verified that

$$\begin{split} b_{1n}^m &= \frac{1}{\lambda + 2\mu} \frac{\mathrm{i} \kappa_p}{2} \int_{R'}^R t^2 W_n^p(R', t) \zeta_n^m(t) \mathrm{d}t \\ &= \frac{1}{\lambda + 2\mu} \frac{\mathrm{i} \kappa_p}{2} \frac{1}{2n + 1} \int_{R'}^R t^2 W_n^p(R', t) \bigg\{ \int_t^R \Big[-n \Big(\frac{t}{\tau} \Big)^{-n - 1} - (n + 1) \Big(\frac{t}{\tau} \Big)^n \Big] \xi_{3n}^m(\tau) \\ &- \sqrt{n(n + 1)} \Big[\Big(\frac{t}{\tau} \Big)^{-n - 1} - \Big(\frac{t}{\tau} \Big)^n \Big] \xi_{1n}^m(\tau) \mathrm{d}\tau \bigg\} \mathrm{d}t. \end{split}$$

We have from (4.11) that

$$\begin{split} b^m_{2n} &= \frac{\mathrm{i} \kappa_s}{2\mu} \int_{R'}^R t^2 W^s_n(R',t) Z^m_{2n}(t) \mathrm{d}t \\ &= \frac{1}{2n+1} \frac{\mathrm{i} \kappa_s}{2\mu} \int_{R'}^R t^2 W^s_n(R',t) \bigg\{ \int_t^R \sqrt{n(n+1)} (c_2 - c_4) \xi^m_{3n}(\tau) \\ &+ \left[(n+1)c_2 + nc_4 \right] \xi^m_{1n}(\tau) \mathrm{d}\tau \bigg\} \mathrm{d}t \\ &= \frac{1}{2n+1} \frac{\mathrm{i} \kappa_s}{2\mu} \int_{R'}^R t^2 W^s_n(R',t) \bigg\{ \int_t^R \sqrt{n(n+1)} \Big[\Big(\frac{t}{\tau} \Big)^{-n-1} - \Big(\frac{t}{\tau} \Big)^n \Big] \xi^m_{3n}(\tau) \\ &+ \Big[(n+1) \Big(\frac{t}{\tau} \Big)^{-n-1} + n \Big(\frac{t}{\tau} \Big)^n \Big] \xi^m_{1n}(\tau) \, \mathrm{d}\tau \bigg\} \mathrm{d}t. \end{split}$$

It follows from (4.12) that

$$\begin{split} b^m_{3n} &= \frac{\mathrm{i} \kappa_s}{2 \mu R R'} \int_{R'}^R t^3 W^s_n(R',t) Z^m_{3n}(t) \mathrm{d}t \\ &= \frac{\mathrm{i} \kappa_s}{2 \mu R R'} \frac{1}{2n+1} \int_{R'}^R t^3 W^s_n(R',t) \bigg\{ \int_t^R \sqrt{n(n+1)} (c_1 - c_3) \xi^m_{2n}(\tau) \mathrm{d}\tau \bigg\} \mathrm{d}t \\ &= \frac{\mathrm{i} \kappa_s}{2 \mu R R'} \frac{1}{2n+1} \int_{R'}^R t^3 W^s_n(R',t) \\ &\quad \times \bigg\{ \int_t^R \sqrt{n(n+1)} \Big[\Big(\frac{t}{\tau}\Big)^{-n-2} - \Big(\frac{t}{\tau}\Big)^{n-1} \Big] \xi^m_{2n}(\tau) \mathrm{d}\tau \bigg\} \mathrm{d}t. \end{split}$$

Substituting (4.9)–(4.12) into (4.25), we obtain

$$\begin{split} d^m_{1n} &= -\frac{2\kappa_s}{\pi \mu R'} \int_{R'}^R t^2 S^s_n(t) Z^m_{2n}(t) \mathrm{d}t \\ &= -\frac{2\kappa_s}{\pi \mu R'} \frac{1}{2n+1} \int_{R'}^R t^2 S^s_n(t) \bigg\{ \int_t^R \sqrt{n(n+1)} \Big[\Big(\frac{t}{\tau}\Big)^{-n-1} - \Big(\frac{t}{\tau}\Big)^n \Big] \xi^m_{3n}(\tau) \\ &+ \Big[(n+1) \Big(\frac{t}{\tau}\Big)^{-n-1} + n \Big(\frac{t}{\tau}\Big)^n \Big] \xi^m_{1n}(\tau) \mathrm{d}\tau \bigg\} \mathrm{d}t, \end{split}$$

$$\begin{split} d_{2n}^{m} &= -\frac{1}{\sqrt{n(n+1)}} \frac{R'}{\mu} Z_{3n}^{m}(R') \\ &= -\frac{1}{\sqrt{n(n+1)}} \frac{R'}{\mu} \frac{1}{2n+1} \int_{R'}^{R} \sqrt{n(n+1)} \left[\left(\frac{R'}{\tau} \right)^{-n-2} - \left(\frac{R'}{\tau} \right)^{n-1} \right] \xi_{2n}^{m}(\tau) d\tau, \end{split}$$

and

$$d_{3n}^{m} = \frac{1}{\lambda + 2\mu} \frac{2\kappa_{p}}{\pi R'} \int_{R'}^{R} t^{2} S_{n}^{p}(t) \zeta_{n}^{m}(t) dt$$

$$= \frac{1}{\lambda + 2\mu} \frac{2\kappa_{p}}{\pi R'} \frac{1}{2n+1} \int_{R'}^{R} t^{2} S_{n}^{p}(t) \left\{ \int_{t}^{R} \left[-n \left(\frac{t}{\tau} \right)^{-n-1} - (n+1) \left(\frac{t}{\tau} \right)^{n} \right] \xi_{3n}^{m}(\tau) - \sqrt{n(n+1)} \left[\left(\frac{t}{\tau} \right)^{-n-1} - \left(\frac{t}{\tau} \right)^{n} \right] \xi_{1n}^{m}(\tau) d\tau \right\} dt.$$

For sufficiently large n, it is shown in Lemma 4.4 and [3] that

$$||Q_n|| \lesssim n \left(\frac{R'}{R}\right)^n, \quad ||\overline{K_n(R)}\overline{M_{\text{diag}}}|| \lesssim n \left(\frac{R'}{R}\right)^n, \quad |W_n(R',t)| \lesssim \frac{1}{n} \left(\frac{t}{R'}\right)^n.$$

Substituting the above estimates into \boldsymbol{b}_n^m and \boldsymbol{d}_n^m leads to

$$\left|b_{jn}^m\right| \lesssim \frac{1}{n^2} \left(\frac{R}{R'}\right)^n \|\boldsymbol{\xi}\|_{L^{\infty}([R',R])}, \quad \left|d_{jn}^m\right| \lesssim \frac{1}{n^2} \left(\frac{R}{R'}\right)^n \|\boldsymbol{\xi}\|_{L^{\infty}([R',R])}.$$

Hence we have from (4.26) that

$$\begin{aligned} |\boldsymbol{p}_{n}^{m}(R)| &\leq \left|\overline{Q_{n}}\boldsymbol{p}_{n}^{m}(R')\right| + \left|\overline{Q_{n}}\boldsymbol{d}_{n}^{m}\right| + \left|\overline{K_{n}(R)}\overline{M_{\operatorname{diag}}}\boldsymbol{b}_{n}^{m}\right| \\ &\lesssim n\left(\frac{R'}{R}\right)^{n}\sum_{i=1}^{3}|p_{in}^{m}(R')| + \frac{1}{n}\|\boldsymbol{\xi}\|_{L^{\infty}([R',R])} + \frac{1}{n}\|\boldsymbol{\xi}\|_{L^{\infty}([R',R])}, \end{aligned}$$

which completes the proof.

LEMMA 4.9. Let p be the solution of the dual problem (4.6). For sufficiently large N, the following estimate holds:

$$\left| \int_{\Gamma_R} \left(\mathscr{T} - \mathscr{T}_N \right) \boldsymbol{\xi} \cdot \overline{\boldsymbol{p}} \right| \, \mathrm{d}s \lesssim \frac{1}{N} \| \boldsymbol{\xi} \|_{\boldsymbol{H}^1(\Omega)}^2.$$

Proof. It is shown in [27] that all the elements of the DtN matrix M_n have an order n. Hence,

$$\left| \int_{\Gamma_{R}} (\mathscr{T} - \mathscr{T}_{N}) \boldsymbol{\xi} \cdot \overline{\boldsymbol{p}} \, \mathrm{d}s \right| \leq \left| \sum_{n=N+1} \sum_{|m| \leq n} M_{n} \boldsymbol{\xi}(R) \cdot \overline{\boldsymbol{p}}(R) \right|$$

$$\leq \sum_{n=N+1} \sum_{|m| \leq n} n \left(|\xi_{1n}^{m}(R)| + |\xi_{2n}^{m}(R)| + |\xi_{3n}^{m}(R)| \right)$$

$$\times \overline{\left(|p_{1n}^{m}(R)| + |p_{2n}^{m}(R)| + |p_{3n}^{m}(R)| \right)}$$

$$\lesssim \sum_{n=N+1} \left[n \left(1 + n(n+1) \right)^{1/2} \right]^{-1/2} \left[\sum_{|m| \leq n} \left(1 + n(n+1) \right)^{1/2} \right]$$

$$\times \left(|\xi_{1n}^{m}(R)|^{2} + |\xi_{2n}^{m}(R)|^{2} + |\xi_{3n}^{m}(R)|^{2} \right) \right]^{1/2}$$

$$\times \left[\sum_{|m| \leq n} n^{3} \left(|p_{1n}^{m}(R)|^{2} + |p_{2n}^{m}(R)|^{2} + |p_{3n}^{m}(R)|^{2} \right) \right]^{1/2}$$

$$\lesssim \frac{1}{N} \|\boldsymbol{\xi}\|_{\boldsymbol{H}^{1/2}(\Gamma_{R})} \left[\sum_{n=N+1} \sum_{|m| \leq n} n^{3} \left(|p_{1n}^{m}(R)|^{2} + |p_{2n}^{m}(R)|^{2} + |p_{3n}^{m}(R)|^{2} \right) \right]^{1/2}$$

$$(4.27) \quad \lesssim \frac{1}{N} \|\boldsymbol{\xi}\|_{\boldsymbol{H}^{1}(\Omega)} \left[\sum_{n=N+1} \sum_{|m| \leq n} n^{3} \left(|p_{1n}^{m}(R)|^{2} + |p_{2n}^{m}(R)|^{2} + |p_{3n}^{m}(R)|^{2} \right) \right]^{1/2}.$$

It follows from Lemma 4.8 that

$$\begin{split} &\sum_{n=N+1} \sum_{|m| \le n} n^3 \left(|p_{1n}^m(R)|^2 + |p_{2n}^m(R)|^2 + |p_{3n}^m(R)|^2 \right) \\ &\lesssim \sum_{n=N+1} \sum_{|m| \le n} n^3 \left[n^2 \left(\frac{R'}{R} \right)^{2n} \sum_{i=1}^3 |p_{in}^m(R')|^2 + \frac{1}{n^2} \|\boldsymbol{\xi}\|_{L^{\infty}([R',R])}^2 \right] \\ &\lesssim \sum_{n=N+1} \sum_{|m| \le n} n^5 \left(\frac{R'}{R} \right)^{2n} \sum_{i=1}^3 |p_{in}^m(R')|^2 + \sum_{n=N+1} \sum_{|m| \le n} (1 + n(1+n))^{1/2} \|\boldsymbol{\xi}\|_{L^{\infty}([R',R])}^2 \\ &:= J_1 + J_2. \end{split}$$

Noting that the function t^4e^{-2t} is bounded on $(0, +\infty)$, we have

$$J_1 \lesssim \max_{n=N+1} \left(n^4 \left(\frac{R'}{R} \right)^{2n} \right) \sum_{n=N+1} \sum_{|m| < n} n \sum_{i=1}^3 |p_{in}^m(R')|^2 \lesssim \|\boldsymbol{p}\|_{H^{1/2}(\Gamma_{R'})}^2 \lesssim \|\boldsymbol{\xi}\|_{\boldsymbol{H}^1(\Omega)}.$$

It is shown in [21] that

$$\begin{split} &\|\xi_{j}^{m}(t)\|_{L^{\infty}([R',R])}^{2} \leq \left(\frac{2}{R-R'}+n\right)\|\xi_{jn}^{m}(t)\|_{L^{2}([R',R])}^{2}+\frac{1}{n}\|\xi_{jn}^{m'}(t)\|_{L^{2}([R',R])}^{2}, \\ &\|\xi_{jn}^{m}\|_{H^{1}(B_{R}\backslash B_{R'})}^{2} \geq \int_{R'}^{R}\left[\left(R'+\frac{n^{2}}{R}\right)|\xi_{jn}^{m}(\rho)|^{2}+R'\left|\xi_{jn}^{m'}(\rho)\right|^{2}\right]\mathrm{d}\rho. \end{split}$$

Substituting them into J_2 gives

$$J_{2} \lesssim \sum_{n=N+1} \sum_{|m| \leq n} (1 + n(1+n))^{1/2}$$

$$\times \sum_{j=1}^{3} \left[\left(\frac{2}{R-R'} + n \right) \|\xi_{jn}^{m}(t)\|_{L^{2}([R',R])}^{2} + \frac{1}{n} \|\xi_{jn}^{m'}(t)\|_{L^{2}([R',R])}^{2} \right]$$

$$\lesssim \|\xi\|_{H^{1}(B_{R} \setminus B_{R'})}^{2} \leq \|\xi\|_{H^{1}(\Omega)}^{2},$$

which yields

$$\sum_{n=N+1} \sum_{|m| \le n} n^3 \left(|p_{1n}^m(R)|^2 + |p_{2n}^m(R)|^2 + |p_{3n}^m(R)|^2 \right) \lesssim \|\boldsymbol{\xi}\|_{\boldsymbol{H}^1(\Omega)}^2.$$

Plugging the above estimate into (4.27), we obtain

$$\left| \int_{\Gamma_R} \left(\mathscr{T} - \mathscr{T}_N \right) \boldsymbol{\xi} \cdot \overline{\boldsymbol{p}} \mathrm{d}s \right| \lesssim \frac{1}{N} \| \boldsymbol{\xi} \|_{\boldsymbol{H}^1(\Omega)}^2,$$

which completes the proof.

We are now in position to show the proof of Theorem 4.1.

Proof. It follows from (4.2) that

$$\begin{aligned} \|\boldsymbol{\xi}\|_{\boldsymbol{H}^{1}(\Omega)}^{2} &= \Re b(\boldsymbol{\xi}, \boldsymbol{\xi}) + \Re \int_{\Gamma_{R}} (\mathscr{T} - \mathscr{T}_{N}) \boldsymbol{\xi} \cdot \overline{\boldsymbol{\xi}} ds + 2\omega^{2} \int_{\Omega} \boldsymbol{\xi} \cdot \overline{\boldsymbol{\xi}} d\boldsymbol{x} + \Re \int_{\Gamma_{R}} \mathscr{T}_{N} \boldsymbol{\xi} \cdot \overline{\boldsymbol{\xi}} ds \\ &\leq C_{1} \left[\left(\sum_{T \in M_{h}} \eta_{T}^{2} \right)^{1/2} + N \left(\frac{R'}{R} \right)^{N} \|\boldsymbol{u}^{\text{inc}}\|_{\boldsymbol{H}^{1}(\Omega)} \right] \|\boldsymbol{\xi}\|_{\boldsymbol{H}^{1}(\Omega)} \\ &+ \left(C_{2} + C(\delta) \right) \|\boldsymbol{\xi}\|_{\boldsymbol{L}^{2}(\Omega)}^{2} + \left(\frac{R}{R'} \right) \delta \|\boldsymbol{\xi}\|_{\boldsymbol{H}^{1}(\Omega)}^{2}. \end{aligned}$$

Choosing δ such that $\frac{R}{\hat{R}} \frac{\delta}{\min(\mu,\omega^2)} < \frac{1}{2}$, we get

$$\|\boldsymbol{\xi}\|_{\boldsymbol{H}^{1}(\Omega)}^{2} \leq 2C_{1} \left[\left(\sum_{T \in M_{h}} \eta_{T}^{2} \right)^{1/2} + N \left(\frac{R'}{R} \right)^{N} \|\boldsymbol{u}^{\text{inc}}\|_{\boldsymbol{H}^{1}(\Omega)} \right] \|\boldsymbol{\xi}\|_{\boldsymbol{H}^{1}(\Omega)}$$

$$+ 2 \left(C_{2} + C(\delta) \right) \|\boldsymbol{\xi}\|_{\boldsymbol{L}^{2}(\Omega)}^{2}.$$
(4.28)

Using Lemmas 4.3, 4.5, and 4.9 yields

$$\begin{split} \|\boldsymbol{\xi}\|_{\boldsymbol{L}^{2}(\Omega)}^{2} &= b(\boldsymbol{\xi}, \boldsymbol{p}) + \int_{\Gamma_{R}} \left(\mathscr{T} - \mathscr{T}_{N} \right) \boldsymbol{\xi} \cdot \overline{\boldsymbol{p}} \mathrm{d}s - \int_{\Gamma_{R}} \left(\mathscr{T} - \mathscr{T}_{N} \right) \boldsymbol{\xi} \cdot \overline{\boldsymbol{p}} \mathrm{d}s \\ &\lesssim \left[\left(\sum_{T \in M_{h}} \eta_{T}^{2} \right)^{1/2} + N \left(\frac{R'}{R} \right)^{N} \|\boldsymbol{u}^{\mathrm{inc}}\|_{\boldsymbol{H}^{1}(\Omega)} \right] \|\boldsymbol{\xi}\|_{H^{1}(\Omega)} + \frac{1}{N} \|\boldsymbol{\xi}\|_{H^{1}(\Omega)}^{2}. \end{split}$$

Substituting the above estimate into (4.28) and taking sufficiently large N such that

$$\frac{2\left(C_2 + C(\delta)\right)}{N} \frac{1}{\min(\mu, \omega^2)} < 1,$$

we obtain

$$\|\boldsymbol{u} - \boldsymbol{u}_N^h\|_{\boldsymbol{H}^1(\Omega)} \lesssim \left(\sum_{T \in M_h} \eta_T^2\right)^{1/2} + N\left(\frac{R'}{R}\right)^N \|\boldsymbol{u}^{\text{inc}}\|_{\boldsymbol{H}^1(\Omega)},$$

which completes the proof.

- 1. Given the tolerance $\epsilon > 0, \theta \in (0, 1)$;
- 2. Fix the computational domain $\Omega = B_R \setminus \overline{D}$ by choosing the radius R;
- 3. Choose R' and N such that $\epsilon_N \leq 10^{-8}$;
- 4. Construct an initial mesh \mathcal{M}_h over Ω and compute error estimators;
- 5. While $\epsilon_h > \epsilon$ do
- 6. Refine the mesh \mathcal{M}_h according to the strategy:

if
$$\eta_{\hat{T}} > \theta \max_{T \in \mathcal{M}_h} \eta_T$$
, then refine the element $\hat{T} \in \mathcal{M}_h$;

- 7. Solve the discrete problem (3.3) on the new mesh which is still denoted as \mathcal{M}_h ;
- 8. Compute the corresponding error estimators;
- 9. End while
- 5. Implementation and numerical experiments. In this section, we discuss the algorithmic implementation of the adaptive finite element DtN method and present two numerical examples to demonstrate the effectiveness of the proposed method.
- 5.1. Adaptive algorithm. Based on the a posteriori error estimate in Theorem 4.1, we adopt FreeFem [18] to implement the adaptive algorithm of the linear finite elements. By Theorem 4.1, the a posteriori error estimator consists of three parts: the first two parts are related to the finite element discretization error ϵ_h , and the third part is the DtN truncation error ϵ_N , which depends on the truncation number N. Explicitly,

$$\epsilon_h = \left(\sum_{T \in \mathcal{M}_h} \eta_T^2\right)^{1/2}, \quad \epsilon_N = N\left(\frac{R'}{R}\right)^N \|\boldsymbol{u}^{\mathrm{inc}}\|_{\boldsymbol{H}^1(\Omega)}.$$

In the implementation, the parameters R', R, and N are chosen such that the finite element discretization error is not polluted by the DtN truncation error; i.e., ϵ_N is required to be very small compared to ϵ_h , for example, $\epsilon_N \leq 10^{-8}$. For simplicity, in the following numerical experiments, R' is chosen such that the obstacle is exactly contained in the ball $B_{R'}$, and N is taken to be the smallest positive integer such that $\epsilon_N \leq 10^{-8}$. Table 1 shows the algorithm of the adaptive finite element DtN method for solving the elastic obstacle scattering problem.

5.2. TBC matrix construction. Denote by $\{\Psi_j\}_{j=1}^L$ the basis of the finite element space V_h . Then the finite element approximation of the solution is

(5.1)
$$\mathbf{u}_N = \sum_{i=1}^L u_i \mathbf{\Psi}_i.$$

Recall that the truncated DtN operator (3.1) is

$$\mathscr{T}_N \boldsymbol{u}_N = \sum_{n=0}^N \sum_{m=-n}^n \left\{ \left[M_{11}^{(n,m)} u_{1n}^m(R) + M_{13}^{(n,m)} u_{3n}^m(R) \right] \boldsymbol{U}_n^m + M_{22}^{(n,m)} u_{2n}^m(R) \boldsymbol{V}_n^m \right\}$$

(5.2)
$$+ \left[M_{31}^{(n,m)} u_{1n}^m(R) + M_{33}^{(n,m)} u_{3n}^m(R) \right] X_n^m e_\rho \bigg\},$$

where

$$(5.3) (u_{1n}^m(R), u_{2n}^m(R), u_{3n}^m(R))^{\top} = \int_{\Gamma_R} \boldsymbol{u}_N \cdot \left(\overline{\boldsymbol{U}}_n^m, \overline{\boldsymbol{V}}_n^m, \left(\overline{\boldsymbol{X}}_n^m \boldsymbol{e}_{\rho} \right) \right)^{\top} \mathrm{d}s.$$

Substituting (5.1) into (5.3) yields

$$(5.4) \qquad \left(u_{1n}^m(R), u_{2n}^m(R), u_{3n}^m(R)\right)^{\top} = \sum_{j=1}^L u_j \int_{\Gamma_R} \mathbf{\Psi}_j \cdot \left(\overline{\mathbf{U}_n^m}, \overline{\mathbf{V}_n^m}, \left(\overline{X_n^m} \mathbf{e}_{\rho}\right)\right)^{\top} \mathrm{d}s.$$

Define the components of the vectors $\Phi_U^{(n,m)},\,\Phi_V^{(n,m)},\,$ and $\Phi_X^{(n,m)}$ as follows:

$$\left(\Phi_{U,j}^{(n,m)},\Phi_{V,j}^{(n,m)},\Phi_{X,j}^{(n,m)}\right) = \int_{\Gamma_R} \mathbf{\Psi}_j \cdot \left(\mathbf{U}_n^m, \mathbf{V}_n^m, (X_n^m \mathbf{e}_\rho)\right) \mathrm{d}s.$$

Denote by B the TBC matrix. It follows from (5.2) and (5.4) that

$$\begin{split} \sum_{j=1}^{L} B_{ij} u_{j} &= \int_{\Gamma_{R}} \mathscr{T}_{N} \boldsymbol{u}_{N} \cdot \boldsymbol{\Psi}_{i} \mathrm{d}s \\ &= \sum_{n=0}^{N} \sum_{m=-n}^{n} \bigg\{ \bigg[M_{11}^{(n,m)} \sum_{j} u_{j} \overline{\Phi_{U,j}^{(n,m)}} + M_{13}^{(n,m)} \sum_{j} u_{j} \overline{\Phi_{X,j}^{(n,m)}} \bigg] \Phi_{U,i}^{(n,m)} \\ &+ \bigg[M_{31}^{(n,m)} \sum_{j} u_{j} \overline{\Phi_{U,j}^{(n,m)}} + M_{33}^{(n,m)} \sum_{j} u_{j} \overline{\Phi_{X,j}^{(n,m)}} \bigg] \Phi_{X,i}^{(n,m)} \\ &+ M_{22}^{(n,m)} \sum_{j} u_{j} \overline{\Phi_{V,j}^{(n,m)}} \Phi_{V,i}^{(n,m)} \bigg\}, \end{split}$$

which indicates that the TBC matrix is a low rank matrix constructed by vector products. Specifically, we have

$$B = \sum_{n=0}^{N} \sum_{m=-n}^{n} \left(M_{11}^{(n,m)} \Phi_{U}^{(n,m)} \Phi_{U}^{(n,m)^{*}} + M_{13}^{(n,m)} \Phi_{U}^{(n,m)} \Phi_{X}^{(n,m)^{*}} + M_{22}^{(n,m)} \Phi_{V}^{(n,m)} \Phi_{V}^{(n,m)} + M_{31}^{(n,m)} \Phi_{X}^{(n,m)} \Phi_{U}^{(n,m)^{*}} + M_{33}^{(n,m)} \Phi_{X}^{(n,m)} \Phi_{X}^{(n,m)^{*}} \right)$$
(5.5)

To simplify the notation, define matrices U and V as

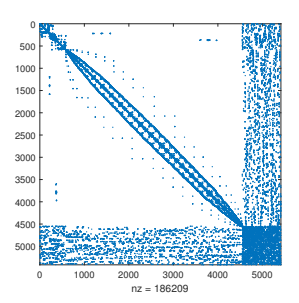
$$\begin{split} U &= \left(\Phi_{U}^{(n,m)}, \Phi_{U}^{(n,m)}, \Phi_{V}^{(n,m)}, \Phi_{X}^{(n,m)}, \Phi_{X}^{(n,m)}, \Phi_{X}^{(n,m)}\right)_{(n,m)}, \\ V &= \left(M_{11}^{(n,m)} \Phi_{U}^{(n,m)^*}, M_{13}^{(n,m)} \Phi_{X}^{(n,m)^*}, M_{22}^{(n,m)} \Phi_{V}^{(n,m)^*}, \\ M_{31}^{(n,m)} \Phi_{U}^{(n,m)^*}, M_{33}^{(n,m)} \Phi_{X}^{(n,m)^*}\right)_{(n,m)}. \end{split}$$

Then we have from (5.5) that

$$(5.6) B = UV.$$

Denote by A the stiffness matrix corresponding to the variational problem with the Neumann condition $\mathcal{D}\mathbf{u} = 0$ on Γ_R and the Dirichlet boundary condition on ∂D , which has the sesquilinear form

$$\hat{b}(\boldsymbol{u}, \boldsymbol{v}) = \mu \int_{\Omega} \nabla \boldsymbol{u} : \nabla \overline{\boldsymbol{v}} \, d\boldsymbol{x} + (\lambda + \mu) \int_{\Omega} (\nabla \cdot \boldsymbol{u}) (\nabla \cdot \overline{\boldsymbol{v}}) \, d\boldsymbol{x} - \omega^2 \int_{\Omega} \boldsymbol{u} \cdot \overline{\boldsymbol{v}} \, d\boldsymbol{x}.$$



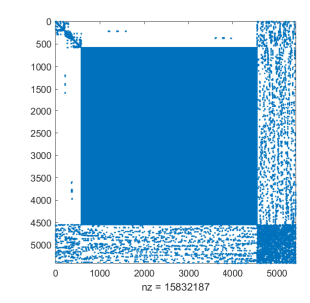


Fig. 1. Sparsity pattern of the coefficient matrix. Left: Matrix A. Right: Matrix W.

Then the stiffness matrix W for the variational problem (3.3) takes the form

$$(5.7) W = A - B.$$

Since the DtN operator is nonlocal, it is clear to note from (5.6) that the nonzeros of B and A are $O(h^{-4})$ and $O(h^{-3})$, respectively. Figure 1 plots the sparsity patterns of matrices A and W with 1805 nodal points in the mesh. Hence, the bandwidth of matrix W is much larger than the bandwidth of matrix A. For the above reason, we do not assemble matrix W and solve the resulting linear system directly.

The matrix A is sparse, real, and symmetric. It can be handled effectively by many parallel direct solvers. Since B is a low rank matrix given in (5.6), the linear system Wz = b can be solved effectively via the generalized Woodbury matrix identity by using the following steps: (1) construct matrices U and V; (2) solve $Az_1 = b$ with a parallel direct solver; (3) perform matrix-vector product $z_2 = Vz_1$; (4) construct matrices $C = A^{-1}U$ and H = I + VC; (5) solve a dense but small-size linear system $Hz_3 = z_2$; (6) perform matrix-vector product $z_4 = Cz_3$; (7) construct the solution of the system Wz = b by $z = z_1 - z_4$. The above approach has several advantages: (1) it is only needed to store matrices A, U and V. The nonzeros of U, V are $O(h^{-2})$; (2) the bandwidth of matrix A is much smaller, so it is faster to solve $Az_1 = b$. Once the linear solver is set up, the construction of matrix $C = A^{-1}U$ is very fast.

Remark 5.1. In the algorithm, it is crucial to accurately compute the Fourier coefficients (5.4), especially for high frequency modes under coarse meshes. Since our focus in this paper is on the a posteriori error estimate, we do not intend to elaborate on this aspect and leave it as future work. We refer the reader to [12, 34, 37] and the references cited therein for the related work.

5.3. Numerical examples. We present two examples to show the performance of the proposed method. In the first example, the obstacle is a ball so that the explicit solution is available. The incident wave is chosen as the third column of the Green tensor. By comparing the numerical solution with the explicit solution, we are able to report the accuracy of the proposed algorithm. In the second example, we consider a more complex geometry: a rectangular U-shaped obstacle. The obstacle is assumed to be illuminated by a compressional plane wave. We pay particular attention to the mesh refinement around the corners of the obstacle, where the solution has singularity. In both examples, the a posteriori error is plotted against the number of unknowns in order to show the convergence rate.

Example 1. In this example, we intend to test the accuracy of the proposed algorithm. The obstacle is taken as a ball with radius 0.5. The TBC is set on the

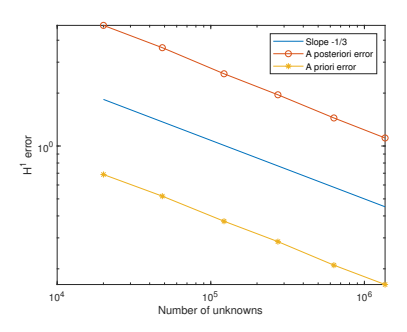


Fig. 2. Example 1. Quasi-optimality of the a priori and a posteriori error estimates.

sphere Γ_R with radius R=1. Denote by $G(x,y;\omega)$ the Green tensor of the three-dimensional elastic wave equation. More explicitly, we have

$$\boldsymbol{G}(\boldsymbol{x},\boldsymbol{y};\omega) = \frac{1}{\mu}g(\boldsymbol{x},\boldsymbol{y};\kappa_s)\boldsymbol{I} + \frac{1}{\omega^2}\nabla_{\boldsymbol{x}}\nabla_{\boldsymbol{x}}^{\top}\left(g(\boldsymbol{x},\boldsymbol{y};\kappa_s) - g(\boldsymbol{x},\boldsymbol{y};\kappa_p)\right),$$

where \boldsymbol{I} is the 3×3 identity matrix and $g(\boldsymbol{x},\boldsymbol{y};\kappa)=\frac{1}{4\pi}\frac{e^{\mathrm{i}\kappa|\boldsymbol{x}-\boldsymbol{y}|}}{|\boldsymbol{x}-\boldsymbol{y}|}$ is the fundamental solution of the three-dimensional Helmholtz equation. The incident wave is chosen as a multiple of the third column of the Green tensor, i.e.,

$$\boldsymbol{u}^{\mathrm{inc}}(\boldsymbol{x};\boldsymbol{y}) = 10\boldsymbol{G}(\boldsymbol{x},\boldsymbol{y};\omega)(:,3),$$

where the source point $\boldsymbol{y}=(0,0,0)^{\top}$ is taken as the origin, the angular frequency $\omega=\pi$, and the Lamé parameters $\mu=1,\lambda=2$. Then it is easy to check that the scattered field is $\boldsymbol{u}=-\boldsymbol{u}^{\text{inc}}$.

Denote the a priori error by $e_h = \|\boldsymbol{u} - \boldsymbol{u}_N^h\|_{\boldsymbol{H}^1(\Omega)}$. Figure 2 displays the curves of $\log e_h$ and $\log \epsilon_h$ against $\log \operatorname{DoF}_h$ for the adaptive mesh refinements, where DoF_h stands for the degrees of freedom or the number of knowns for the mesh \mathcal{M}_h . The red circle line represents the a posteriori error estimate, and the yellow star line stands for the a priori error estimate; the slope of the straight blue line is -1/3 (color available online). It indicates that the meshes and the associated numerical complexity are quasi-optimal; i.e., $\|\boldsymbol{u} - \boldsymbol{u}_N^h\|_{\boldsymbol{H}^1(\Omega)} = O(\operatorname{DoF}_h^{-1/3})$ holds asymptotically.

Example 2. This example demonstrates that the method can handle the problem where the solution has singularity. We consider a more complex geometry: a rectangular U-shaped obstacle, which is shown on the left of Figure 3. In this example, the parameters of the rectangular U-shaped geometry are L=1, D=0.6, H=W=0.2. The obstacle is assumed to be illuminated by a compressional plane wave

$$u^{\text{inc}}(\boldsymbol{x};\boldsymbol{d}) = \boldsymbol{d}e^{\mathrm{i}\kappa_p \boldsymbol{x}\cdot \boldsymbol{d}},$$

where $d = (0, -1, 0)^{\top}$ is the incident direction, the angular frequency $\omega = \pi$, and the Lamé parameters $\mu = 1, \lambda = 2$. Thus the compressional wavenumber $\kappa_p = \pi/2$. The TBC is set on the sphere Γ_R with radius R = 1. Figure 3 plots the curves of $\log \epsilon_h$ versus $\log \text{DoF}_h$ for the adaptive mesh refinements. The blue circle line represents for the a posteriori error estimate, and the red line is a straight line with slope -1/3 (color available online). Again, it indicates that the meshes and the associated numerical complexity are quasi-optimal. Figure 4 shows the initial mesh (1805 nodal points) and the refined mesh after 2 iterative steps with 13352 nodal points. It is clear to

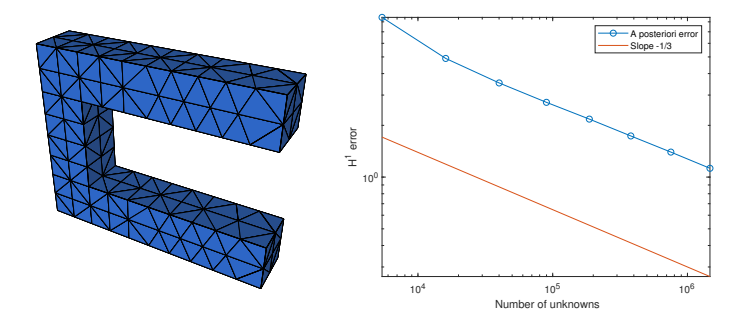


Fig. 3. Example 2: Quasi-optimality of the a posteriori error estimates.

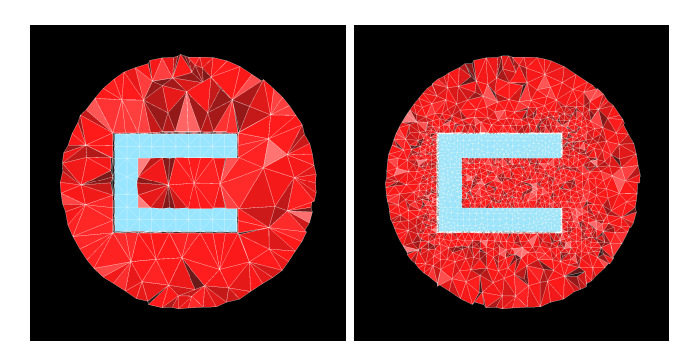


Fig. 4. Example 2: Cross sections of the initial mesh (left) and refined mesh (right).

note that the mesh is refined mainly around the corners and the interior part of the U-shaped obstacle, where the solution has singularity, and stays relatively coarse near the TBC surface, where the solution is smooth.

6. Conclusion. In this paper, we have presented an adaptive finite element DtN method for the elastic obstacle scattering problem in three dimensions. Based on the Helmholtz decomposition, a new duality argument is developed to obtain the a posteriori error estimate. It not only takes into account the finite element discretization error but also includes the truncation error of the DtN operator. We show that the truncation error decays exponentially with respect to the truncation parameter. The a posteriori error estimate for the solution of the discrete problem serves as a basis for the adaptive finite element approximation. Numerical results show that the proposed method is accurate and effective.

REFERENCES

- [1] I. Babuška and A. Aziz, Survey lectures on the mathematical foundations of the finite element method, in The Mathematical Foundations of the Finite Element Method with Applications to Partial Differential Equations, A. Aziz, ed., Academic Press, New York, 1972, pp. 1–359.
- [2] G. BAO, G. Hu, J. Sun, and T. Yin, Direct and inverse elastic scattering from anisotropic media, J. Math. Pures Appl., 117 (2018), pp. 263–301.
- [3] G. BAO, M. ZHANG, B. HU, AND P. LI, An adaptive finite element DtN method for the threedimensional acoustic scattering problem, Discrete Contin. Dyn. Syst. Ser. B, 26 (2021), pp. 61-79
- [4] G. BAO, M. ZHANG, X. JIANG, P. LI, AND X. YUAN, An Adaptive Finite Element DtN Method for the Electromagnetic Scattering Problem, preprint.

- [5] A. BAYLISS AND E. TURKEL, Radiation boundary conditions for numerical simulation of waves, Comm. Pure Appl. Math., 33 (1980), pp. 707-725.
- [6] J. H. Bramble, J. E. Pasciak, and D. Trenev, Analysis of a finite PML approximation to the three dimensional elastic wave scattering problem, Math. Comp., 79 (2010), pp. 2079–2101.
- [7] Z. CHEN, X. XIANG, AND X. ZHANG, Convergence of the PML method for elastic wave scattering problems, Math. Comp., 85 (2016), pp. 2687–2714.
- [8] P. G. Ciarlet, Mathematical Elasticity, Vol. I: Three-Dimensional Elasticity, Stud. Math. Appl. 20, North-Holland, Amsterdam, 1988.
- [9] D. COLTON AND R. KRESS, Integral Equation Methods in Scattering Theory, Wiley, New York, 1983.
- [10] D. COLTON AND R. KRESS, Inverse Acoustic and Electromagnetic Scattering Theory, Springer-Verlag, Berlin, 1998.
- [11] B. ENGQUIST AND A. MAJDA, Absorbing boundary conditions for the numerical simulation of waves, Math. Comp., 31 (1977), pp. 629-651.
- [12] A. FOURNIER, Exact calculation of Fourier series in nonconforming spectral-element methods,
 J. Comput. Phys., 215 (2006), pp. 1–5.
- [13] G. K. GÄCHTER AND M. J. GROTE, Dirichlet-to-Neumann map for three-dimensional elastic waves, Wave Motion, 37 (2003), pp. 293–311.
- [14] D. GIVOLI AND J. B. KELLER, Non-reflecting boundary conditions for elastic waves, Wave Motion, 12 (1990), pp. 261–279.
- [15] M. GROTE AND J. B. KELLER, On nonreflecting boundary conditions, J. Comput. Phys., 122 (1995), pp. 231–243.
- [16] M. GROTE AND C. KIRSCH, Dirichlet-to-Neumann boundary conditions for multiple scattering problems, J. Comput. Phys., 201 (2004), pp. 630–650.
- [17] T. HAGSTROM, Radiation boundary conditions for the numerical simulation of waves, in Acta Numerica 1999, Acta Numer. 8, Cambridge University Press, Cambridge, UK, 1999, pp. 47– 106.
- [18] F. HECHT, New development in FreeFem++, J. Numer. Math., 20 (2012), pp. 251-265.
- [19] G. C. HSIAO, N. NIGAM, J. E. PASIAK, AND L. XU, Error analysis of the DtN-FEM for the scattering problem in acoustic via Fourier analysis, J. Comput. Appl. Math., 235 (2011), pp. 4949–4965.
- [20] G. Hu, A. Rathsfeld, and T. Yin, Finite element method to fluid-solid interaction problems with unbounded periodic interfaces, Numer. Methods Partial Differ. Equations, 32 (2016), pp. 5–35.
- [21] X. JIANG, P. LI, J. LV, AND W. ZHENG, An adaptive finite element method for the wave scattering with transparent boundary condition, J. Sci. Comput., 72 (2017), pp. 936–956.
- [22] X. JIANG, P. LI, J. LV, Z. WANG, H. WU, AND W. ZHENG, An adaptive edge finite element DtN method for Maxwell's equations in biperiodic structures, IMA J. Numer. Anal., (2021), drab052, https://doi.org/10.1093/imanum/drab052.
- [23] X. JIANG, P. LI, AND W. ZHENG, Numerical solution of acoustic scattering by an adaptive DtN finite element method, Commun. Comput. Phys., 13 (2013), pp. 1277–1244.
- [24] L. D. LANDAU AND E. M. LIFSHITZ, Theory of Elasticity, 3rd ed., Pergamon Press, Oxford, UK, 1986.
- [25] M. LENOIR, Optimal isoparametric finite elements and error estimates for domains involving curved boundaries, SIAM J. Numer. Anal., 23 (1986), pp. 562–580, https://doi.org/10. 1137/0723036.
- [26] P. LI, Y. WANG, Z. WANG, AND Y. ZHAO, Inverse obstacle scattering for elastic waves, Inverse Problems, 32 (2016), 115018.
- [27] P. LI AND X. Yuan, Inverse obstacle scattering for elastic waves in three dimensions, Inverse Probl. Imaging, 13 (2019), pp. 545–573.
- [28] P. LI AND X. YUAN, Convergence of an Adaptive Finite Element DtN Method for the Elastic Wave Scattering Problem, preprint, https://arxiv.org/abs/1903.03606, 2019.
- [29] Y. LI, W. ZHENG, AND X. ZHU, A CIP-FEM for high-frequency scattering problem with the truncated DtN boundary condition, CSIAM Trans. Appl. Math., 1 (2020), pp. 530–560.
- [30] L. MA, J. SHEN, L. WANG, AND Z. YANG, Wavenumber explicit analysis for time-harmonic Maxwell equations in a spherical shell and spectral approximation, IMA J. Numer. Anal., 38 (2018), pp. 810–851.
- [31] P. Monk, Finite Element Methods for Maxwell's Equations, Oxford University Press, Oxford, UK, 2003.
- [32] J.-C. Nédélec, Acoustic and Electromagnetic Equations Integral Representations for Harmonic Problems, Springer-Verlag, New York, 2001.

- [33] A. H. Schatz, An observation concerning Ritz-Galerkin methods with indefinite bilinear forms, Math. Comp., 28 (1974), pp. 959–962.
- [34] B. WANG, L. WANG, AND Z. XIE, Accurate calculation of spherical and vector spherical harmonic expansions via spectral element grids, Adv. Comput. Math., 44 (2018), pp. 951–985.
- [35] Z. WANG, G. BAO, J. LI, P. LI, AND H. WU, An adaptive finite element method for the diffraction grating problem with transparent boundary condition, SIAM J. Numer. Anal., 53 (2015), pp. 1585–1607, https://doi.org/10.1137/140969907.
- [36] L. Xu and T. Yin, Analysis of the Fourier series Dirichlet-to-Neumann boundary condition of the Helmholtz equation and its application to finite element methods, Numer. Math., 147 (2021), pp. 967–996.
- [37] Z. YANG, L. WANG, Z. RONG, B. WANG, AND B. ZHANG, Seamless integration of global Dirichlet-to-Neumann boundary condition and spectral elements for transformation electromagnetics, Comput. Methods Appl. Mech. Engrg.,301 (2016), pp. 137–163.
- [38] X. Yuan, G. Bao, and P. Li, An adaptive finite element DtN method for the open cavity scattering problems, CSIAM Trans. Appl. Math., 1 (2020), pp. 316–345.